Ethylene Analogues of Tetrathiafulvalene and Tetraselenafulvalene: New Donors for Organic Metals

Toyonari Sugimoto,* Hiroshi Awaji, Iwao Sugimoto, Yohji Misaki, Tokuzo Kawase, Shigeo Yoneda, and Zen-ichi Yoshida*

Department of Synthetic Chemistry, Kyoto University, Yoshida, Kyoto 606, Japan

Tsunetoshi Kobayashi*

Institute of Physical and Chemical Research, Wako, Saitama 351-01, Japan

Hiroyuki Anzai*

Electrotechnical Laboratory, Tsukuba, Ibaraki 305, Japan

Received February 3, 1989

The following ethylene analogues of tetrathiafulvalene (TTF) and tetraselenafulvalene (TSF) were synthesized for use as new donors for organic metals: ethanediylidene-2,2′-bis(1,3-dithiole) (**1a**), 2-butene-1,4-diylidene-2,2′-bis(1,3-dithiole) (**2a**), ethanediylidene-2,2′-bis(1,3-diselenole) (**3a**), ethanediylidene-2-(1,3-dithiole)-2′-(1,3-diselenole) (**4a**), and their substituted derivatives. The longest wavelength absorption bands in their electronic spectra are shifted to longer wavelength with an increasing number of sp^2 carbon atoms inserted between the two 1,3-dithiole rings and to shorter wavelength with increasing substitution of selenium atoms for sulfur atoms. The characterization of their electronic transitions was made by using Pariser–Parr–Pople (PPP) type SCF calculations with configuration interaction. All the donors exhibited either two-step one-electron or one-step two-electron transfer. From comparison of the redox potentials with those of TTF and TSF, it was shown that **1a**, **3a**, and **4a** are better donors than TTF and that **2a** is comparable with TSF in donating ability. Except for **4a**, the new donors formed charge-transfer (CT) complexes with 7,7,8,8-tetracyanoquinodimethane (TCNQ) and its 2,5-dimethyl-substituted derivative (DMTCNQ), and the room-temperature electric conductivities of the complexes in the compressed pellet states were relatively high (σ_{max} 0.8 S/cm). With use of a diffusion technique, the **1a**–TCNQ complex was obtained as single crystals. The electric conductivity of these crystals was 16 S/cm at 300 K and increased with decreasing temperature to ca. 200 K (23 S/cm).

Introduction

For the past several years, studies on the synthesis and characterization of organic conducting materials (organic metals) have been actively carried out[1] on the basis of the theoretical prediction that superconductivity might occur in organic solids under technologically useful conditions of normal pressure and liquid nitrogen temperatures.[2] In fact, some organic compounds, $(TMTSF)_2X$ (TMTSF = tetramethyltetraselenafulvalene; X = PF_6, AsF_6, SbF_6, TaF_6, ClO_4, ReO_4, FSO_3),[3] (BEDT-TTF))$_4$(ReO_4)$_2$[4] (BEDT-TTF = bis(ethylenedithio)tetrathiafulvalene), (BEDT-TTF)$_2$$I_3$,[5] (BEDT-TTF)$_2$$IBr_2$,[6] (BEDT-TTF)$_2$Cu(NCS)$_2$,[7] and (dimethyl(ethylenedithio)diselenadithiafulvalene)$_2$X (X = $Au(CN)_2$, $AuCl_2$, $AuBr_2$, AuI_2, I_3, IBr_2),[8] have been found to become superconductors, albeit at low temperatures (T_{max} 10.4 K) under normal or high pressure. The stabilization of a superconducting state at still higher temperatures in the future might be attained by using cation radical salts of new tetrathia- (TTF) and tetraselenafulvalene (TSF) derivatives. On the other hand, it seems likely that the creation of novel donors having skeletal structures different from those of TTF and TSF

Scheme I

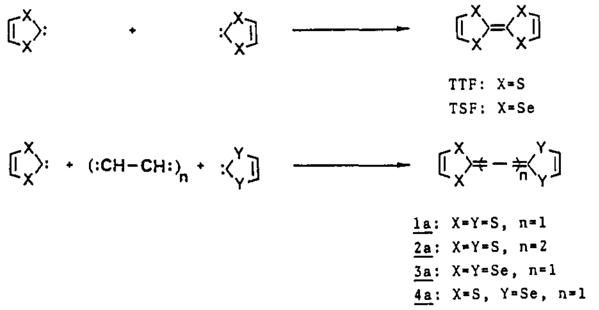

---

[1] See reviews: (a) Garito, A. F.; Heeger, A. J. *Acc. Chem. Res.* **1974**, *7*, 232. (b) Narita, M.; Pittman, C. U. Jr. *Synthesis* **1976**, 489. (c) Torrance, J. B. *Acc. Chem. Res.* **1979**, *12*, 79. (d) Bechgaard, K.; Jérome, D. *Sci. Am.* **1982**, *247*, 50. (e) Bryce, M. R.; Murphy, L. C. *Nature* **1984**, *309*, 119. (f) Maugh, T. H., II *Science* **1983**, *222*, 606. (g) Wudl, F. *Acc. Chem. Res.* **1984**, *17*, 227.

[2] Little, W. A. *Phys. Rev.* **1964**, *A134*, 1416.

[3] (a) Bechgaard, K.; Jacobsene, C. S.; Mortensen, K.; Pedersene, H. J.; Thorup, N. *Phys. Rev.* **1980**, *33*, 1119. (b) Jerome, D.; Mazaud, A.; Riboult, M.; Bechgaard, K. *J. Phys. Lett.* (*Paris*) **1980**, *41*, 95. (c) Jerome, D. *Chem. Scr.* **1981**, *17*, 13. (d) Parkin, S. S. P.; Riboult, M.; Jerome, D.; Bechgaard, K. *J. Phys.* **1981**, *C14*, 5305. (e) Bechgaard, K.; Carneiro, K.; Rasmussen, F. B.; Olsen, M.; Rindorf, G.; Jacobsen, C. S.; Pedersene, H. J.; Scott, J. C. *J. Am. Chem. Soc.* **1981**, *103*, 2440. (f) Parkin, S. S. P.; Jerome, D.; Bechgaard, K. *Mol. Cryst. Liq. Cryst.* **1982**, *79*, 213.

[4] Parkin, S. S. P.; Engler, E. M.; Schumaker, R. R.; Lafier, R.; Lee, V. Y.; Scott, J. C.; Green, R. L.; *Phys. Rev. Lett.* **1983**, *50*, 270.

[5] (a) Yagubskii, E. B.; Shchegolev, I. F.; Laukhin, V. N.; Kononovich, P. A.; Karatsovnik, M. W.; Zvarykina, A. V.; Buravov, L. I. *JETP. Lett.* **1984**, *39*, 12. (b) Kaminskii, V. F.; Prokhorova, T. G.; Shibaeva, R. P.; Yagubskii, E. B. *JETP. Lett.* **1984**, *39*, 17. (c) William, J. M.; Emge, T. J.; Wang, H. H.; Carlson, K. D.; Crabtree, G. W. *Inorg. Chem.* **1984**, *23*, 2558. (d) Crabtree, G. W.; Carlson, K. D.; Hall, L. N.; Copps, P. T.; Wang, H. H.; Emge, T. J.; Beno, M. A.; Williams, J. M. *Phys. Rev.* **1984**, *B30*, 2958. (e) Leung, P. C.; Emge, T. J.; Beno, M. A.; Wang, H. H.; Williams, J. M.; Petricek, V.; Coppens, P. *J. Am. Chem. Soc.* **1984**, *106*, 7644.

[6] (a) Williams, J. M.; Wang, H. H.; Beno, M. A.; Emge, T. J.; Sowa, L. M.; Copps, P. T.; Behroozi, F.; Hall, L. N.; Carlson, K. D.; Crabtree, G. W. *Inorg. Chem.* **1984**, *23*, 3841. (b) Yagubskii, E. B.; Shchegolev, I. F.; Shibaeva, R. P.; Fedutin, D. N.; Rosenberg, L. P.; Sogomonyan, E. M.; Lobkovskaya, R. M.; Laukin, V. N.; Ignat'ev, A. A.; Zvarykina, A. V.; Buravov, L. I. *JETP. Lett.* **1985**, *42*, 206. (c) Heidmann, C. P.; Veith, H.; Andres, K.; Fuchs, H.; Polborn, K.; Amberger, E. *Solid State Commun.* **1986**, *57*, 161.

[7] Urayama, H.; Yamochi, H.; Saito, G.; Nozawa, K.; Sugano, T.; Kinoshita, M.; Sato, S.; Oshima, K.; Kawamoto, A.; Tanaka, J. *Chem. Lett.* **1988**, 55.

[8] Kikuchi, K.; Kikuchi, M.; Namiki, T.; Saito, K.; Ikemoto, I.; Murata, K.; Ishiguro, T.; Kobayashi, K. *Chem. Lett.* **1987**, 931.

0897-4756/89/2801-0535$01.50/0

will be required for the ultimate accomplishment of high-temperature superconductors. In this context, the molecular design and synthesis of new types of donors are of interest to many scientists. However, most of the work so far reported has been confined to the modification of TTF and TSF by introducing appropriate substituents into the TTF and TSF molecular skeletons.

In this paper, we describe the synthesis of the new donors **1a**–**4a** which have formally the structures obtained by inserting two or four sp^2 carbons between two 1,3-dichalcogenole rings, 1,3-dithiole and/or 1,3-diselenole rings (Scheme I). The ^1H and ^{13}C NMR spectra, electronic spectra, and redox behavior of these donors are compared with those exhibited by the reference compounds, TTF and TSF, which have no sp^2 carbons between the dichalcogenole rings.

The rational that led to the design of the above donors was that the radical cation and dication states responsible for electric conduction in the charge-transfer (CT) and radical cation types of organic conducting materials should be significantly stabilized as a result of decreased repulsion of positive charges in more remote positions. However, other essential factors including the stacking mode, intra- and intercolumn interactions, etc., must, of course, also be taken into account. The new donors showed lower first and second oxidation potentials as compared with those of TTF and TSF. Furthermore, these donors react with the acceptors TCNQ and DMTCNQ to provide CT complexes whose electric properties were investigated in both the compressed pellet and single crystalline states.

Experimental Section

General Techniques. Each solvent used in this experiment was purified by distillation over the following drying agents: THF from $LiAlH_4$, benzene from Na–benzophenone, CH_2Cl_2 and acetonitrile from CaH_2, and CCl_4 from $CaCl_2$. Column chromatography was carried out on silica gel (Wacogel C-200) or neutral alumina (deactivated Woelm N Akt I with 1 wt % water). Melting points were determined by using either a Büchi melting-point apparatus in sealed capillary tubes or a Yanaco micromelting-point apparatus and are uncorrected. Spectra were recorded with the following instruments: ^1H NMR spectra with either a JEOL Model PMX 60 (60 MHz) or JEOL Model FX 90Q (90 MHz) with Me_4Si as internal standard; ^{13}C NMR spectra with either a JEOL Model JNM-GX400 (operating at 100 MHz) or JEOL Model FX 90Q (operating at 22.5 MHz); infrared spectra with either a JASCO A-102 or a Hitachi grating infrared spectrophotometer Model EPI-G3; electronic spectra with a Hitachi 340 spectrophotometer or a Varian spectrophotometer Cary; mass spectra with a JEOL Model JMS-DX 300 spectrometer; ESR spectra with a JEOL Model PE-3X spectrometer. Elemental analyses were carried out at the Elemental Analytical Center of Kyoto University.

Materials. The following compounds were prepared according to the methods described in the literature cited: 1,3-dithiolylium tetrafluoroborate,[9] 4,5-dimethyl-1,3-dithiolylium perchlorate,[10] 4,5-diphenyl-1,3-dithiolylium perchlorate,[10] 1,3-benzodithiolylium tetrafluoroborate,[11] 1,4-butenediylidene-2,2′-bis(4,5-dicarbomethoxy-1,3-dithiole) (**2b**),[12] 2,2′-diphenyl-1,4-butenediylidene-2,2′-bis(4,5-dicarbomethoxy-1,3-dithiole) (**2f**),[12] and 1,4-cyclohexenylidene-2,2′-bis(4,5-dicarbomethoxy-1,3-dithiole) (**2h**).[13]

Electrochemical Measurements. The cyclic voltammery system used in this work was composed of Yanaco voltammetric analyzer Model P-1000, Watanabe X–Y recorder Model WX 4401, and Yanaco function generator Model FG-121B. All measurements were carried out at 25 °C under N_2 atomosphere. Tetraethylammonium perchlorate, which was used as a supporting electrolyte, was recrystallized twice from ethyl acetate and dried for 5 h at 100 °C and 10^{-2} Torr. The voltammetric cell contained a Pt wire working and counter electrode and reference (Ag/AgCl) electrodes. The concentrations of sample and supporting electrolyte were 1 mg/10 mL and 0.1 M, respectively.

Electric Conductivity Measurement. The room-temperature conductivity and activation energy of the compressed pellets were measured by using a four-probe method for **1a**-TCNQ, **1i**-TCNQ, **2i**-TCNQ, $(\mathbf{3a})_2$-$(TCNQ)_3$, $(\mathbf{4a})_2$-$(TCNQ)_3$, and **1a**-DMTCNQ complexes and a two-probe method for **1a**-TCNQ, **1c**-$(DMTCNQ)_{0.72}$, **1i**-TCNQ, **3a**-TCNQ and **4a**-DMTCNQ, at the Institute of Molecular Science. We also used the four-probe method to examine the electrical properties of **1a**-TCNQ single crystals at the Electrotechnical Laboratory. The activation energies, E_a, were evaluated from the following equation:

$$\log R = \log R_0 + (E_a \log e)/(10^3 k)(1000/T)$$

where R is the resistance, T, the temperature, and k, the Boltzmann constant. The slope (A) of the straight line obtained by plotting log R with respect to $1000/T$ is equivalent to $(E_a \log e)/(10^3 k)$. Therefore, E_a can be obtained by the following equation:

$$E_a = (10^3 kA)/(\log e)$$

Computations. The PPP type SCF-MO-CI calculations were carried out for the π systems of TTF, TSF, **1a**, **2a**, **3a**, and **4a** on a Facom M-380 computer at the Institute of Physical and Chemical Research. The atomic and molecular parameter sets required in the calculations were taken from ref 14a for carbon and sulfur atoms and from ref 14b for the selenium atom, respectively. In the configuration interaction (CI) calculations, all the singly excited configurations among the π orbitals were taken into account. The geometrical structural data for TTF were taken from ref 15, and the geometrical structure of TSF was assumed from the data for tetramethyltetraselenafulvalene (TMTSF) reported in ref 16. The bond angles and lengths of the central olefinic moieties of **1a**, **3a**, and **4a** were assumed to be the same as those of *trans*-1,3-butadiene[17] and those of **2a** were derived from the data for *trans*-1,3,5-hexatriene.[18] The dimensions of the terminal five-membered rings of **1a**, **2a**, **3a**, and **4a** were assumed to be the same as those in TTF and/or TMTSF.

General Procedure for the Preparation of (1,3-Dithiolyl)tributylphosphonium Salts (5a, 5c, and 5d). Tri-*n*-butylphosphine (10 mmol) was added to a solution of 1,3-dithiolylium tetrafluoroborate, 4,5-dimethyl-1,3-dithiolylium perchlorate, 4,5-diphenyl-1,3-dithiolylium perchlorate, or 1,3-benzodithiolylium tetrafluoroborate (10 mmol) in acetonitrile (70 mL). The solution was continuously stirred at room temperature, and after 30 min the solvent was evaporated in vacuo to afford a residue ranging from syrupy to solid. Recrystallization from acetonitrile–ether gave **5a**, **5c**, and **5d** in 80–100% yield.

(1,3-Dithiol-2-yl)tri-*n*-butylphosphonium tetrafluoroborate (5a): yield 100%; a light-brown syrupy oil; ^1H NMR (CD_3CN) δ 0.7–2.7 (m, 27 H, *n*-Bu), 6.17 (d, 1 H, $J_{^{31}P-H} = 2$ Hz, 1 H, methine), 6.28 (s, 2 H, ring); IR (neat) 3060, 2950, 2860, 1465, 1050 cm^{-1}.

(4,5-Dimethyl-1,3-dithiol-2-yl)tri-*n*-butylphosphonium perchlorate (5c): yield 90%; colorless crystals; mp 113–114 °C; ^1H NMR (CD_3CN) δ 1.90 (s, 6 H, Me), 0.7–2.6 (m, 27 H, *n*-Bu), 5.62 (d, $J_{^{31}P-H} = 2$ Hz, 1 H, *methine*); IR (KBr) 2900, 1460, 1090 cm^{-1}.

---

(9) Wudl, F.; Kaplan, M. L.; Hufnagel, E. J.; Southwick, E. W., Jr. *J. Org. Chem.* **1974**, *39*, 3608.

(10) (a) Takamizawa, A.; Hirai, K. *Chem. Pharm. Bull.* **1969**, *17*, 1924. (b) Bechgaard, K.; Cowan, D. O.; Bloch, A. N. *J. Org. Chem.* **1975**, *40*, 746.

(11) Nakayama, J.; Fujiwara, K.; Hoshino, M. *Bull. Chem. Soc. Jpn.* **1976**, *49*, 3567.

(12) Mckinnon, D. M.; Buchshriber, J. M. *Can J. Chem.* **1971**, *49*, 3299.

(13) (a) Ishikawa, K.; Akiba, K.; Inamoto, N. *Tetrahedron Lett.* **1976**, 3695. (b) Sato, M.; Gonnella, N. C.; Cava, M. P. *J. Org. Chem.* **1979**, *44*, 930.

(14) (a) Fabian, J.; Mehlhorn, A.; Zahradník, R. *J. Phys. Chem.* **1968**, *72*, 3975. (b) Fabian, J.; Mehlhorn, A.; Zahradník, R. *Theor. Chim. Acta* **1968**, *12*, 247.

(15) Cooper, W. F.; Kenny, N. C.; Edmonds, J. W.; Nagel, A.; Wudl, F.; Coppens, P. *J. Chem. Soc., Chem. Commun.* **1971**, 889.

(16) Kistenmacher, T. J.; Emge, T. J.; Shu, P.; Cowan, D. O. *Acta Crystallogr.* **1979**, *B35*, 772.

(17) Almenningen, A.; Bastiansen, O.; Traetteberg, M. *Acta Chem. Scand.* **1958**, *12*, 1221.

(18) Traetteberg, M. *Acta Chem. Scand.* **1968**, *22*, 628.

(4,5-Diphenyl-1,3-dithiol-2-yl)tri-*n*-butylphosphonium perchlorate (5d): yield 80%; colorless crystals; ^1H NMR (CD_3CN) δ 1.9–2.3 (m, 27 H, *n*-Bu), 5.85 (d, $J_{^{31}P-H}$ = 2 Hz, 1 H, methine), 7.38 (m, 10 H, Ar); IR (KBr) 3050, 2950, 1460, 1440, 1140, 1120, 1080, 740 cm^{-1}.

2-(Formylmethylene)-1,3-dithiole (7a). Method A: To a mixture of **5a** (3.92 g, 10 mmol) and 40% aqueous glyoxal (2.90 g, 20 mmol) in THF (60 mL), triethylamine (10 mL) was added dropwise with stirring at room temperature. After stirring for 1 h, the solvent and triethylamine were removed in vacuo to leave a red residue which was twice extracted with dichloromethane (100 mL). The extract was washed with water, dried over Na_2SO_4, followed by concentration in vacuo. The orange residue was chromatographed on silica gel by using dichloromethane as an eluent to give **7a** (1.02g, 71%): orange crystals (from hexane); mp 81–82 °C; ^1H NMR ($CDCl_3$) δ 6.77 (d, 1 H, *J* = 2 Hz, =*CH*—CHO), 6.87 (s, 2 H, ring), 9.40 (d, 1 H, *J* = 2 Hz, =CH—*CH*O); IR (KBr) 3100, 3070, 2840, 2790, 1613, 1594, 1452, 750, 670 cm^{-1}; mass, *m/e* 144 (M^+). Anal. Calcd for $C_5H_4OS_2$: C, 41.65; H, 2.80; O, 11.09; S, 44.46. Found: C, 41.62; H, 2.94; O, 11.35; S, 44.18. Method B: A mixture of **7b** (1.60 g, 6.15 mmol) and excess $LiBr{\cdot}H_2O$ (4.65 g, 44.3 mmol) in HMPA (40 mL) was heated at 95 °C for 1 h and then 155 °C for 1 h under bubbling N_2. The mixture was cooled to room temperature, poured into water, and extracted three times with benzene (200 mL). The benzene extract was washed with water, dried over Na_2SO_4, and concentrated in vacuo. The residue was chromatographed on silica gel by using dichloromethane as an eluent to give **7a** (640 mg, 72%).

2-(Formylmethylene)-4,5-dicarbomethoxy-1,3-dithiole (7b). Method A: The reaction of **5c** (507 mg, 1 mmol) with 40% aqueous glyoxal (290 mg, 2 mmol) in THF (15 mL) in the presence of triethylamine (5 mL) gave **7b** (188 mg, 70%): orange needles (from MeOH); mp 111–112 °C; ^1H NMR ($CDCl_3$) δ 3.93 (s, 6 H, OMe), 6.68 (d, 1 H, *J* = 3 Hz, =*CH*—CHO), 9.48 (d, 1 H, *J* = 3 Hz, =CH—*CH*O); IR (KBr) 2720, 1730, 1630, 1570, 1470, 1250, 1086, 1030, 1010, 895, 750 cm^{-1}; mass, *m/e* 260 (M^+). Anal. Calcd for $C_9H_8O_5S_2$: C, 41.53; H, 3.10; O, 30.73; S, 24.64. Found: C, 41.33; H, 3.07; O, 30.90; S, 24.48. Method B: To a mixture of **5b** (2.03 g, 4 mmol) and glyoxal diethyl acetal (0.53 g, 4 mmol) in THF (40 mL), triethylamine (2 mL) was added dropwise. The same treatment described in the preparation (method A) of **7a** yielded **7b** (0.59 g, 57%).

We also used the same procedure as described for the preparation (method A) of **7a** to prepare the following 2-(formylmethylene)-1,3-dithioles.

2-(Formylmethylene)-4,5-dimethyl-1,3-dithiole (7c): yield 83%; orange crystals (from hexane); mp 51–52 °C; ^1H NMR ($CDCl_3$) δ 2.15 (s, 6 H, Me), 6.60 (d, *J* = 2 Hz, =*CH*—CHO), 9.90 (d, *J* = 2 Hz, =CH—*CH*O); IR (KBr) 2900, 1618 (C=O), 1380, 1280, 1060 cm^{-1}; mass, *m/e* 172 (M^+). Anal. Calcd for $C_7H_8OS_2$: C, 48.81; H, 4.68; O, 9.29; S, 37.22. Found: C, 48.59; H, 4.44; O, 9.17; S, 37.42.

2-(Formylmethylene)-4,5-diphenyl-1,3-dithiole (7d): yield 93%; orange crystals (from MeOH); mp 157–158 °C; ^1H NMR ($CDCl_3$) δ 6.75 (d, 1 H, *J* = 2 Hz, =*CH*—CHO), 7.39 (m, 10 H, Ar), 9.58 (d, 1 H, *J* = 2 Hz, =CH—*CH*O); IR (KBr) 2850, 2800, 1630, 1450, 5380, 1050, 750 cm^{-1}; mass, *m/e* 296 (M^+). Anal. Calcd for $C_{17}H_{12}OS_2$: C, 68.89; H, 4.08; S, 21.63. Found: C, 69.01; H, 3.80; S, 21.90.

2-(Formylmethylene)-1,3-benzodithiole (7e): yield 88%; yellow needles (from MeOH); mp 93–94 °C; ^1H NMR ($CDCl_3$) δ 6.70 (d, 1 H, *J* = 3 Hz, =*CH*—CHO), 7.2–7.7 (m, 4 H, Ar), 9.57 (d, 1 H, *J* = 3 Hz, =CH—*CH*O); IR (KBr) 2770, 2700, 1625, 1470, 1040, 760 cm^{-1}; mass, *m/e* 194 (M^+). Anal. Calcd for $C_8H_6OS_2$: C, 55.64; H, 3.11; O, 8.24; S, 33.01. Found: C, 55.73; H, 3.36; O, 7.94; S, 32.96.

Ethanediylidene-2,2′-bis(4,5-bis(methoxycarbonyl)-1,3-dithiole) (1b). Method A: To a mixture of **5b** (507 mg, 1 mmol) and **7b** (260 mg, 1 mmol) in THF (20 mL), triethylamine (0.5 mL) was added dropwise. The resultant red solution was stirred for 1 h and then evaporated. The residue was washed in hot MeOH and filtered off to give **1b** (337 mg, yield 73%): purple–brown needles (from dichloromethane–hexane); mp 184–185 °C; IR (KBr) 3000, 1716, 1570, 1260, 1080, 1018 cm^{-1}; mass, *m/e* 462 (M^+). Anal. Calcd for $C_{16}H_{14}O_8S_4$: C, 41.55; H, 3.05; O, 27.67; S, 27.73. Found: C, 41.57; H, 3.03; O, 27.47; S, 27.60. Method B: The reaction of **5b** (507 mg, 1 mmol) with 40% aqueous glyoxal (72 mg, 0.5 mmol) in THF (15 mL) containing triethylamine (1 mL) produced **1b** (73 mg, yield 35%) in addition to **7b** (65 mg, yield 32%).

Ethanediylidene-2,2′-bis(4,5-dimethyl-1,3-dithiole) (1c). To a phosphorane solution generated from **5c** (750 mg, 4.36 mmol) with *n*-BuLi (4.36 mmol) in dry THF (20 mL) under argon at −78 °C was added dropwise a solution of **7c** (750 mg, 4.36 mmol) in dry THF (15 mL). After the reaction temperature was gradually raised to room temperature, the resultant yellow solid was filtered off, washed with water and methanol, and dried in vacuo to give crude **1c** (965 mg, yield 78%). Column chromatography on neutral alumina by using benzene as an eluent and subsequent recrystallization from benzene gave pure **1c**: yellow crystals; mp 220–222 °C (dec); IR (KBr) 2900, 1508, 1430, 1270, 800 cm^{-1}; mass, *m/e* 286 (M^+). Anal. Calcd for $C_{12}H_{14}S_4$: C, 50.31; H, 4.93; S, 44.76. Found: C, 50.36; H, 4.93; S, 44.65.

The above procedure was used for the preparation of other ethanediylidene-2,2′-bis(1,3-dithiole)'s.

Ethanediylidene-2,2′-(4,5-diphenyl-1,3-dithiole) (1d): yield 80%; yellow crystals (from benzene); mp 180 °C (dec); IR (KBr) 3050, 1600, 1515, 1440, 740 cm^{-1}; mass, *m/e* 534 (M^+). Anal. Calcd for $C_{32}H_{22}S_4$: C, 71.87; H, 4.15; S, 23.98. Found: C, 71.68; H, 4.04; S, 23.90.

Ethanediylidene-2,2′-bis(1,3-benzodithiole) (1e): yield 70%; pale yellow crystals (from chloroform); mp 200 °C (dec); IR (KBr) 3050, 1505, 1460, 805 cm^{-1}; mass, *m/e* 330 (M^+). Anal. Calcd for $C_{16}H_{10}S_4$: C, 58.14; H, 3.50; S, 33.81. Found: C, 58.42, H, 3.29; S, 33.60. When triethylamine was used as a base in place of *n*-BuLi in the above reaction, the yield decreased to 30%.

Ethanediylidene-2-(4,5-dicarbomethoxy-1,3-dithiole)-2′-(1,3-benzodithiole) (1f): yield 46%; brown needles (from dichloromethane–hexane); mp 134–135 °C; IR (KBr) 1730, 1710, 1575, 1563, 1420, 1280, 1250, 1028 cm^{-1}; mass, *m/e* 396 (M^+). Anal. Calcd for $C_{16}H_{12}O_4S_4$: C, 48.46; H, 3.05; O, 16.14; S, 32.35. Found: C, 48.35; H, 3.33; O, 16.37; S, 32.09.

Ethanediylidene-2-(4,5-dimethyl-1,3-dithiole)-2′-(4,5-dicarbomethoxy-1,3-dithiole) (1h): yield 71%; purple–brown needles (from dichloromethane–hexane); mp 147–148 °C; IR (KBr) 2990, 2940, 2920, 2890, 1705, 1695, 1562, 1548, 1510, 1412, 1265, 1089, 1035, 783, 699 cm^{-1}; mass, *m/e* 374 (M^+). Anal. Calcd for $C_{14}H_{14}O_4S_4$: C, 44.91; H, 3.77; S, 34.24. Found: C, 44.66; H, 3.79; S, 34.02.

Ethanediylidene-2-(4,5-dimethyl-1,3-dithiole)-2′-(1,3-benzodithiole) (1j): yield 69%; yellow needles (from benzene); mp 202–203 °C; IR (KBr) 3030, 2890, 2825, 1509, 1440, 1407, 1280, 1267, 1119, 800, 732, 673 cm^{-1}; mass, *m/e* 308 (M^+). Anal. Calcd for $C_{14}H_{12}S_4$: C, 54.51; H, 3.92; S, 41.57. Found: C, 54.38; H, 3.89; S, 41.42.

Ethanediylidene-2,2′-bis(1,3-dithiole) (1a). The reaction of **1b** (445 mg, 0.963 mmol) with excess $LiBr{\cdot}H_2O$ (1.0 g, 9.52 mmol) in HMPA (15 mL) afforded **1a** (169 mg, yield 86%): yellow crystals (from benzene); mp 164–165 °C (dec); IR (KBr) 3070, 1580, 1534, 1495, 1280, 1240, 1081, 900, 860, 800, 660 cm^{-1}; mass, *m/e* 230 (M^+). Anal. Calcd for $C_8H_6S_4$: C, 41.70; H, 2.63; S, 55.67. Found: C, 41.83; H, 2.54; O, 55.42.

Ethanediylidene-2-(1,3-dithiole)-2′-(1,3-benzodithiole) (1g). The reaction of **1f** (200 mg, 0.505 mmol) with excess $LiBr{\cdot}H_2O$ (600 mg, 5.71 mmol) in HMPA (14 mL) gave **1g** (109 mg, yield 77%): yellow crystals (from benzene–hexane); mp 126–127 °C; IR (KBr) 1560, 1535, 1510 (C=C), 1442, 1430, 1117, 800 cm^{-1}; mass, *m/e* 280 (M^+). Anal. Calcd for $C_{12}H_8S_4$: C, 51.39; H, 2.88; S, 45.73. Found: C, 51.21; H, 2.99; S, 45.51.

Ethanediylidene-2-(4,5-dimethyl-1,3-dithiole)-2′-(1,3-dithiole) (1i). The reaction of **1h** (400 mg, 1.07 mmol) with excess $LiBr{\cdot}H_2O$ (980 mg, 9.33 mmol) in HMPA (14 mL) gave **1i** (237 mg, yield 86%): yellow crystals (from benzene); mp 151–152 °C (dec); IR (KBr) 3050, 2880, 1529, 1504, 1267, 1180, 1080, 800, 787 cm^{-1}; mass, *m/e* 258 (M^+). Anal. Calcd for $C_{10}H_{10}S_4$: C, 46.48; H, 3.90; S, 49.62. Found: C, 46.60; H, 4.03; S, 49.32.

1,4-But-2-enediylidene-2,2′-bis(1,3-dithiole) (2a). Method A: The reaction of **2b**[17] (97 mg, 0.20 mmol) and excess $LiBr{\cdot}H_2O$ (400 mg, 3.81 mmol) in HMPA (14 mL) gave **2a** (16 mg, yield 31%): mp 118–120 °C (dec); IR (KBr) 1565, 1322, 960, 805 cm^{-1}; mass, *m/e* 256 (M^+). Anal. Calcd for $C_{10}H_8S_4$: C, 46.84; H, 3.14; S, 50.02. Found: C, 46.71; H, 3.31; S, 49.75. Method B: $LiAlH_4$ (109 mg, 2.87 mmol) was added to a solution of $TiCl_4$ (0.688 mL, 6.27 mmol) in dry THF (10 mL) under argon, and the mixture was refluxed for 15 min. To the above solution was added a mixture of **7a** (182 mg, 1.26 mmol) and tri-*n*-butylamine (0.302 mL) in dry THF (10 mL). After refluxing for 1 h, the mixture was treated with 20% aqueous potassium carbonate and extracted with benzene. The filtrate was washed with water, dried over sodium sulfate, and concentrated in vacuo. The residue was chromatographed on neutral alumina by using benzene as an eluent to give **2a** (89 mg, yield 55%).

The two procedures used for the preparation of **2a** were also applied to the preparation of other 1,4-butenediylidene-2,2′-bis(1,3-dithiole)s.

1,4-But-2-enediylidene-2,2′-bis(4,5-dimethyl-1,3-dithiole) (2c): yield 52% (method B); orange needles (from benzene); mp 176–178 °C (dec); IR (KBr) 3000, 2910, 2850, 1550, 1430, 945, 801, 650 cm^{-1}; mass, *m/e* 312 (M$^+$). Anal. Calcd for $C_{14}H_{16}S_4$: C, 54.03; H, 5.20; S, 41.03. Found: C, 53.81; H, 5.16; S, 40.82.

1,4-But-2-enediylidene-2,2′-bis(4,5-diphenyl-1,3-dithiole) (2d): yield 100% (method B); orange crystals (from dichloromethane–hexane); mp 193–194 °C (dec); IR (KBr) 3025, 1518, 1565, 1546, 1480, 1437, 1311, 935, 740, 690 cm^{-1}; mass, *m/e* 560 (M$^+$). Anal. Calcd for $C_{34}H_{24}S_4$: C, 72.82; H, 4.31; S, 22.87. Found: C, 72.04; H, 4.36; S, 22.50.

1,4-But-2-enediylidene-2,2′-bis(1,3-benzodithiole) (2e): yield 69% (method B); yellow crystals (from benzene); mp 225–227 °C (dec); IR (KBr) 1567, 1440, 1430, 1325, 1115, 950 cm^{-1}; mass, *m/e* 356 (M$^+$). Anal. Calcd for $C_{18}H_{12}S_4$: C, 60.63; H, 3.39; S, 35.97. Found: C, 60.51; H, 3.61; S, 35.77.

1,4-Diphenyl-1,4-but-2-enediylidene-2,2′-bis(1,3-dithiole) (2g): yield 45% (method A); yellow crystals (from benzene); mp 171–172 °C; IR (KBr) 1550, 930, 800, 760, 700 cm^{-1}; mass, *m/e* 404 (M$^+$). Anal. Calcd for $C_{22}H_{16}S_4$: C, 64.66; H, 3.95; S, 31.39. Found: C, 64.69; H, 3.89; S, 31.21.

1,4-Cyclohexenediylidene-2,2′-bis(1,3-dithiole) (2i): yield 68% (method A); orange needles (from hexane); mp 175–176 °C (dec); IR (KBr) 3060, 2920, 1556, 950, 800, 725 cm^{-1}; mass, *m/e* 282 (M$^+$). Anal. Calcd for $C_{12}H_{10}S_4$: C, 51.03; H, 3.57; S, 45.40. Found: C, 51.02; H, 3.48; S, 45.15.

Ethanediylidene-2,2′-bis(1,3-dithiolium) Bromide (1a$^{\bullet+}$Br$^-$). To a solution of **1a** (47 mg, 0.20 mmol) in dry CCl_4 (30 mL) was added dropwise a 0.10 M solution of bromine in CCl_4 (1.0 mL, 0.10 mmol) with stirring at 0 °C. The red–purple solid precipitated was filtered off and washed with dry CCl_4 to give **1a**$^{\bullet+}$Br$^-$ (62 mg, yield 100%): mp > 300 °C; IR (KBr) 3450, 3060, 1440, 1400, 1202, 754, 741, 692 cm^{-1}.

Ethanediylidene-2,2′-bis(4,5-dimethyl-1,3-dithiolium) Bromide (1c$^{\bullet+}$Br$^-$). The reaction of **1c** (11 mg, 0.038 mmol) with a 0.5 equiv of bromine (0.016 mmol) in dry CCl_4 (15 mL) gave **1c**$^{\bullet+}$Br$^-$ as red–purple solids (14 mg, yield 100%): mp 80–81 °C; IR (KBr) 1475, 1400, 1356, 1190, 932, 702 cm^{-1}.

Ethanediylidene-2,2′-bis(1,3-dithiolium) Dibromide (1a^{2+}2Br$^-$). The reaction of **1a** (70 mg, 0.30 mmol) with an equimolar amount of bromine (0.30 mmol) in dry CCl_4 (30 mL) gave **1a**$^{2+}$2Br$^-$ (117 mg, yield 100%) as an orange solid: mp > 300 °C; IR (KBr) 3450, 3050, 1440, 1270, 1237 cm^{-1}.

Ethanediylidene-2,2′-bis(4,5-dimethyl-1,3-dithiolium) Dibromide (1c^{2+}2Br$^-$). The reaction of **1c** (286 mg, 1 mmol) with an equimolar amount of bromine (1 mmol) in dry CCl_4 (85 mL) gave **1c**$^{2+}$2Br$^-$ (446 mg, yield 100%) as an orange solid: mp 113–114 °C (dec); IR (KBr) 3400, 1630, 1495, 1270, 945, 918 cm^{-1}.

1,4-But-2-enediylidene-2,2′-bis(4,5-dimethyl-1,3-dithiolium) Dibromide (2c^{2+}2Br$^-$). The reaction of **2c** (20 mg, 0.064 mmol) with an equimolar amount of bromine (0.064 mmol) in dry CCl_4 (10 mL) gave **2c**$^{2+}$2Br$^-$ (30 mg, yield 100%) as an orange solid: IR (KBr) 3025, 2960, 2910, 1510, 1226, 1087 cm^{-1}.

(4,5-Dicarbomethoxy-1,3-diselenol-2-yl)tri-*n*-butylphosphonium Tetrafluoroborate (8). Freshly distilled tri-*n*-butylphosphine (1.19 g, 5.88 mmol) was added to a solution of carbon diselenide (1.00 g, 5.88 mmol) in dry ether (25 mL) at 0 °C under N_2 atmosphere. The resultant green solution was then cooled to −65 °C. To this solution was added dropwise a mixture of dimethyl acetylenedicarboxylate (852 mg, 5.88 mmol) and fluoroboric acid etherate (1.03 g, 6.36 mmol). The solution immediately turned red, and a gummy red solid precipitated. Prolonged stirring resulted in a pale brown solid which was then filtered off and washed with ether to afford **8** (2.48 g, yield 70%): colorless needles (from acetonitrile–ether); mp 141–142 °C; ^{1}H NMR ($CDCl_3$) δ 0.7–2.8 (m, 27 H, *n*-Bu), 3.86 (s, 6 H, CO_2Me), 5.67 (d, 1 H, $J_{^{31}P-H}$ = 2 Hz, methine); IR (KBr) 2965, 2945, 2875, 1720, 1572, 1460, 1420, 1265, 1232, 1080 cm^{-1}. Anal. Calcd for $C_{19}H_{34}BO_4F_4PSe_2$: C, 37.90; H, 5.69; P, 5.14. Found: C, 37.77; H, 5.84; P, 5.21.

2-(Formylmethylene)-4,5-dicarbomethoxy-1,3-diselenole (9). The reaction of **8** (800 mg, 1.33 mmol) with 40% aqueous glyoxal (386 mg, 1.33 mmol) in THF (40 mL) in the presence of triethylamine (15 mL) gave **9** (397 mg, yield 84%): yellow needles (from MeOH); mp 108–109 °C; ^{1}H NMR ($CDCl_3$) δ 3.91 (s, 3 H, CO_2Me), 3.93 (s, 3 H, CO_2Me), 7.44 (d, 1 H, *J* = 3 Hz, =C*H*—CHO), 9.78 (d, 1 H,j = 3 Hz, =CH—C*H*O); IR (KBr) 3010, 2945, 2865, 1725, 1700, 1609, 1570, 1445, 1428, 1373, 1265, 1240, 1063, 1030, 1010, 780, 750 cm^{-1}; mass, *m/e* 356 (M$^+$, based on ^{80}Se). Anal. Calcd for $C_9H_8O_5Se_2$: C, 30.53; H, 2.28. Found: C, 30.49; H, 2.23.

Ethanediylidene-2,2′-bis(4,5-dicarbomethoxy-1,3-diselenole) (3b). The reaction of **9** (72 mg, 0.20 mmol) with the phosphorane generated from **8** (122 mg, 0.200 mmol) by use of an equimolar *n*-butyllithium solution (0.20 mmol) in dry THF (20 mL) afforded **3b** (79 mg, yield 60%): orange needles (from dichloromethane–hexane); mp 156–157 °C; ^{13}C NMR ($CDCl_3$) δ 53.3 (CO_2Me, $J_{^{13}C-H}$ = 149 Hz), 120.6 (olefinic, 159 Hz), 121.4 (Se-C-Se), 133.2 and 135.0 (Se—C=C—Se), 161.7 and 161.9 (CO_2Me); IR (KBr) 3030, 2970, 1720, 1572, 1431, 1251, 1071, 1009, 906, 760 cm^{-1}; mass, *m/e* 654 (M$^+$, based on ^{80}Se). Anal. Calcd for $C_{16}H_{14}O_8Se_4$: C, 29.56; H, 2.17. Found: C, 29.56; H, 2.14.

Ethanediylidene-2,2′-bis(1,3-diselenole) (3a). The reaction of **3b** (200 mg, 0.308 mmol) and excess LiBr·H_2O (600 mg, 5.71 mmol) in HMPA (14 mL) afforded **3a** (87 mg, yield 68%): yellow crystals (from benzene); mp 183–184 °C (dec); IR (KBr) 3020, 2910, 1535, 1509, 1429, 1269, 1070, 805, 714 cm^{-1}; mass, *m/e* 422 (M$^+$, based on ^{80}Se). Anal. Calcd for $C_8H_6Se_4$: C, 22.99; H, 1.45. Found: C, 23.27; H, 1.62.

Ethanediylidene-2-(4,5-dicarbomethoxy-1,3-dithiole)-2′-(4,5-dicarbomethoxy-1,3-diselenole) (4b). The reaction of a solution of **9** (397 mg, 1.12 mmol) with the phosphorane generated from **5b** (568 mg, 1.12 mmol) using an equimolar *n*-butyllithium solution (1.12 mmol) in dry THF (2 mL) afforded **4b** (583 mg, yield 94%): purple–brown needles (from dichloromethane–hexane); mp 175–176 °C; ^{13}C NMR ($CDCl_3$) δ 53.3 (CO_2Me, $J_{^{13}C-H}$ = 149 Hz), 113.0 (olefinic, $J_{^{13}C-H}$ = 160 Hz), 119.0 (olefinic, $J_{^{13}C-H}$ = 158 Hz), 119.8 (Se-*C*-Se), 120.0 (S-*C*-S), 130.2, 131.9 (S—*C*=*C*—S), 133.1, 135.0 (Se—*C*=*C*—Se), 159.6, 160.0, 161.7, 162.0 (CO_2Me); IR (KBr) 3020, 2990, 2930, 1720, 1690, 1566, 1429, 1240, 1090, 1065, 1023, 1010 cm^{-1}; mass, *m/e* 558 (M$^+$, based on ^{80}Se). Anal. Calcd for $C_{16}H_{14}O_8S_2Se_2$: C, 34.54; H, 2.54. Found: C, 34.49; H, 2.28.

Ethanediylidene-2-(1,3-dithiole)-2′-(1,3-diselenole) (4a). The reaction of **4b** (200 mg, 0.360 mmol) with excess LiBr·H_2O (600 mg, 5.71 mmol) in HMPA (14 mL) afforded **4a** (71 mg, yield 61%): yellow crystals (from benzene); mp 162 °C (dec); IR (KBr) 3030, 1534, 1500, 1272, 800, 720, 655 cm^{-1}; mass, *m/e* 326 (M$^+$, based on ^{80}Se), calcd for $C_8H_6S_2Se_2$ 325.82845, found 325.82345. Anal. Calcd for $C_8H_6S_2Se_2$: C, 29.64;, H, 1.88. Found: C, 30.68; H, 1.86.

General Procedure for the Preparation of Charge-Transfer Salts of the New Donors with TCNQ and DMTCNQ. The donor and acceptor in equimolar amounts were dissolved in separate solvents (acetonitrile was employed for **1a**, **1i**, **2i**, **3a**, and **4a**, and dichloromethane for **1c**). When the two hot solutions were mixed, the charge-transfer salt precipitated immediately. The salt was filtered, washed several times with the solvent used, and dried in vacuo. The ratios of donor and acceptor in the complexes were determined by elemental analyses.

1a–TCNQ: yield 79%; fine purple needles; mp 170–171 °C; IR (KBr) 2187 cm^{-1}. Anal. Calcd for $C_{20}H_{10}N_4S_4$: C, 55.29; H, 2.32; N, 12.89; S, 29.51. Found: C, 55.11; H, 2.19; N, 12.87; S, 29.17.

1c–TCNQ: yield 48%; fine purple crystals with green luster; mp 172–173 °C; IR (KBr) 2175 cm^{-1}. Anal. Calcd for $C_{24}H_{18}N_4S_4$: C, 58.75; H, 3.70; N, 11.42; S, 26.14. Found: C, 58.61; H, 3.48; N, 11.32; S, 25.84.

1i–TCNQ: yield 66%; fine purple needles; mp 141–142 °C; IR (KBr) 2185 cm^{-1}. Anal. Calcd for $C_{22}H_{14}N_4S_4$: C, 57.12; H, 3.05; N, 12.11. Found: C, 57.35; H, 3.10; N, 12.41.

Scheme II

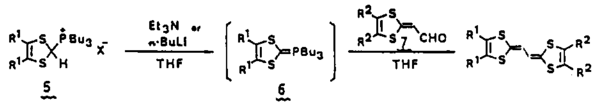

1b: $R^1 = R^2 = CO_2Me$
1c: $R^1 = R^2 = Me$
1d: $R^1 = R^2 = Ph$
1e: $R^1 = R^2 = -(CH{=}CH)_2-$
1f: $R^1 = CO_2Me$, $R^2 = -(CH{=}CH)_2-$
1h: $R^1 = Me$, $R^2 = CO_2Me$
1j: $R^1 = Me$, $R^2 = -(CH{=}CH)_2-$

2i–TCNQ: yield 69%; fine purple needles; mp > 260 °C; IR (KBr) 2188 cm^{-1}. Anal. Calcd for $C_{24}H_{14}N_4S_4$: C, 59.24; H, 2.90; N, 11.51. Found: C, 59.08; H, 2.85; N, 11.25.

(3a)$_2$–(TCNQ)$_3$: yield 73%; dark green needles; mp > 260 °C; IR (KBr) 2196 cm^{-1}. Anal. Calcd for $C_{52}H_{24}N_{12}Se_8$: C, 43.12; H, 1.67; N, 11.60. Found: C, 43.36; H, 1.72; N, 11.76.

(4a)$_2$–(TCNQ)$_3$: yield 66%; dark purple needles; mp > 260 °C; IR (KBr) 2194 cm^{-1}. Anal. Calcd for $C_{52}H_{24}N_{12}S_4Se_4$: C, 49.53; H, 1.92; N, 13.33. Found: C, 48.94; H, 1.95; N, 13.21.

1a–DMTCNQ: yield 75%; fine purple needles; mp 169–170 °C. Anal. Calcd for $C_{22}H_{14}N_4S_4$: C, 57.12; H, 3.05; N, 12.11. Found: C, 57.38; H, 2.90; N, 11.93.

1b–(DMTCNQ)$_{0.72}$: yield 61%; fine purple crystals; mp 185–186 °C. Anal. Calcd for $C_{26}H_{22}N_4S_4$: C, 60.21; H, 4.27; N, 10.80. Found: C, 62.54; H, 4.06; N, 12.77.

1i–DMTCNQ: yield 14%; fine purple needles; mp 158–159 °C. Anal. Calcd for $C_{24}H_{18}N_4S_4$: C, 58.74; H, 3.70; N, 11.42. Found: C, 58.59; H, 3.60; N, 11.43.

2i–DMTCNQ: yield 70%; fine dark green needles; mp 172–173 °C. Anal. Calcd for $C_{20}H_{18}N_4S_4$: C, 60.67; H, 3.52; N, 10.89. Found: C, 60.68; H, 3.53; N, 10.84.

3a–DMTCNQ: yield 60%; dark green needles; mp 189–190 °C. Anal. Calcd for $C_{22}H_{14}N_4Se_4$: C, 40.64; H, 2.17; N, 8.62. Found: C, 40.59; H, 2.10; N, 8.40.

4a–DMTCNQ: yield 48%; dark green needles; mp 165–166 °C. Anal. Calcd for $C_{22}H_{14}N_4S_2Se_2$: C, 47.49; H, 2.54; N, 10.07. Found: C, 47.79; H, 2.53; N, 10.22.

Preparation of 1a–TCNQ Single Crystals. A quartz apparatus was employed that consisted of three chambers connected by a tube leading from the top of the terminal chambers to the side of the center chamber. The total volume of the apparatus was approximately 100 mL. Access to each chamber was provided by ground joints with high-vacuum grease. The center chamber was sealed with a ground-glass stopper. All loading steps were performed in a glovebox purged with nitrogen. The compound **1a** (116 mg, 0.504 mmol) was placed in one chamber, and TCNQ (101 mg, 0.500 mmol) was placed in the other chamber. The apparatus was then carefully filled with anisole (90 mL), sealed, and allowed to stand for 130 days at 20 °C to produce crystals in the center chamber. The crystals were filtered off and washed with anisole several times. the largest single crystal thus obtained was 3 × 0.05 × 0.05 mm^3.

Results and Discussion

Syntheses of Ethanediylidene-2,2′-bis(1,3-dithiole)s (1), Ethanediylidene-2,2′-bis(1,3-diselenole)s (3), and Ethanediylidene-2-(1,3-dithiole)-2′-(1,3-diselenole)s (4). For the syntheses of 1, 3, and 4 we adopted the double Wittig reaction strategy. Thus, the synthesis of 1 was achieved by using the Wittig reactions of (1,3-dithiolidene)phosphoranes (**6**), generated in situ from the corresponding phosphonium salts (**5**),[13] with 2-(formylmethylene)-1,3-dithioles (**7**, Scheme II). 2-(Formylmethylene)-4,5-dicarbomethoxy-1,3-dithiole (**7b**) was provided by the Wittig reaction of phosphonium salt **5b**[13b] with glyoxal diethylsemiacetal[19] in the presence of *n*-BuLi, followed by chromatography on silica gel, as shown in Scheme III. Although the yield of **7b** is fairly good (~60%), this method has a disadvantage in the extra preparation of glyoxal diethylsemiacetal. We found a more convenient method that involves the reaction of **5b** with a commercially available aqueous glyoxal solution (40% in water) in the presence of excess Et_3N. In this case the expected compound **1b** was obtained along with **7b**. When the molar ratio of **5b** and glyoxal was 2:1, **1b** and **7b** were obtained in 32 and 35% yields, respectively. With an equimolar ratio, **7b** was obtained in an increased yield (60%), and the formation of **1b** was suppressed to only 3%. By use of excess aqueous glyoxal (1:2 → 1:10) the yield of **7b** was further improved to 70%, and the formation of **1b** was almost not detected. On the basis of these results, the initial Wittig reaction was carried out at the **5**:glyoxal molar ratio of 1:2 because there is no need to separate **1b** and **7b** and the fact that **7b** can be also utilized for the synthesis of unsymmetrical **1s**. Thus, from the phosphonium salts **5a**, **5c**, **5d**, and **5e**[13a] the corresponding aldehydes **7a**, **7c**, **7d**, and **7e** were obtained in the yields of 71, 83, 92, and 88%, respectively (Table I). The results of the subsequent second Wittig reaction of **5** with **7** are summarized in Table II. The reaction of **7b** with **5b** proceeded readily in the presence of Et_3N to give **1b** in 73% yield. When triethylamine was used in the reaction of **5c** with **7c**, the tetramethyl derivative **1c** was not obtained at all. However, the use of *n*-BuLi gave the expected compound in 66% yield. The dibenzo derivative **1e** was obtained in yields of 30 and 70% by use of Et_3N and *n*-BuLi, respectively. This compound was previously synthesized in our and other laboratories by the deprotonation of bis(1,3-benzodithiolylium)ethene bis(tetrafluoroborate).[20] The present strategy has great advantages in the facile synthesis of unsymmetrical ethanediylidene derivatives. Thus, **1f**, **1h**, and **1j** were obtained in 46, 71, and 69% yields, respectively (see Table II).

Scheme III

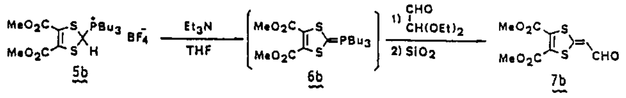

Table I. Synthesis of 2-(Formylmethylene)-1,3-dithioles 7a–e and 9 by the Wittig Reaction of Phosphonium Salts 5a–e and 8 with Glyoxal in the Presence of Triethylamine

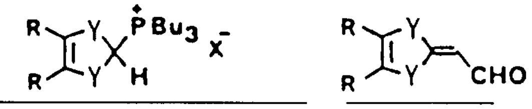

	Y	R	X		yield, %
5a	S	H	BF_4	**7a**	71
5b	S	CO_2Me	BF_4	**7b**	70
5c	S	Me	ClO_4	**7c**	83
5d	S	Ph	ClO_4	**7d**	92
5e	S	$-(CH{=}CH)_2-$	BF_4	**7e**	88
8	Se	CO_2Me	BF_4	**9**	84

The demethoxycarbonylation of **1b**, **1f**, and **1h** was readily achieved by treatment with lithium bromide monohydrate ($LiBr{\cdot}H_2O$) in hot hexamethylphosphoramide (HMPA).[21] Thus, a mixture of the ester and excess $LiBr{\cdot}H_2O$ in HMPA was heated first at 95 °C for 1 h and then at 155 °C for additional 1 h with bubbling nitrogen, and the demethoxycarbonylated products (**1a**,[22] **1g**, and

---

(19) Fisher, E.; Baër, P. *Helv. Chim. Acta* **1935**, *18*, 514.

(20) (a) Kawase, T.; Awaji, H.; Yoneda, S.; Yoshida, Z. *Heterocycles* **1982** *18*, 123. (b) Bryce, M. R. *J. Chem. Soc., Chem. Commun.* **1983**, 4. (c) Bryce, M. R. *J. Chem. Soc., Perkin Trans. 1* **1985**, 1675.

(21) (a) Lakshmikantham, M. V.; Cava, M. P. *J. Org. Chem.* **1976**, *41*, 882. (b) Yoneda, S.; Kawase, T.; Yasuda, Y.; Yoshida, Z. *Ibid.* **1979**, *44*, 1728. (c) Lakshmikantham, M. V.; Cava, M. P. *Ibid.* **1980**, *45*, 2632.

(22) Yoshida, Z.; Kawase, T.; Awaji, H.; Sugimoto, I.; Sugimoto, T.; Yoneda, S. *Tetrahedron Lett.* **1983**, 3469.

Table II. Synthesis of Ethanediylidene Derivatives 1b–f,h,j, 3b, and 4b by the Wittig Reaction of (1,3-Dithiole)phosphonium Salts 5b–e and 8 with the 2-(Formylmethylene)-1,3-dithioles 7b–e and 9 in the Presence of Triethylamine or *n*-BuLi

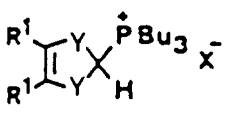 (Y, R^1, X)	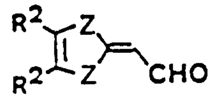 (Z, R^2)	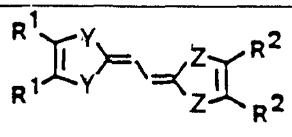 (Y, Z, R^1, R^2)	yield, %
5b: S, CO_2Me, BF_4	**7b**: S, CO_2Me	**1b**: S, S, CO_2Me, CO_2Me	73^a
5c: S, Me, ClO_4	**7c**: S, Me	**1c**: S, S, Me, Me	66^b
5d: S, Ph, ClO_4	**7d**: S, Ph	**1d**: S, S, Ph, Ph	80^b
5e: S, $-(CH{=}CH)_2-$, BF_4	**7e**: S, $-(CH{=}CH)_2-$	**1e**: S, S, $-(CH{=}CH)_2-$, $-(CH{=}CH)_2-$	70^b $(30)^a$
5b: S, CO_2Me, BF_4	**7e**	**1f**: S, S, CO_2Me, $-(CH{=}CH)_2-$	46^a
5c	**7b**	**1h**: S, S, Me, CO_2Me	71^b
5c	**7e**	**1j**: S, S, Me, $-(CH{=}CH)_2-$	69^b
8: Se, CO_2Me, BF_4	**9**: Se, CO_2Me	**3b**: Se, Se, CO_2Me, CO_2Me	60^b
5b	**9**	**4b**: S, Se, CO_2Me, CO_2Me	94^b

^{a} Et_3N as a base. ^{b} *n*-BuLi as a base.

Table III. ^1H NMR Spectral Data (δ) for the New Donors^a

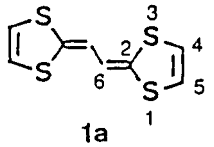 **1a**	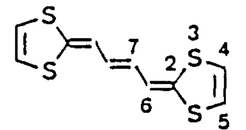 **2a**	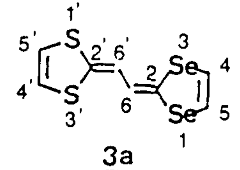 **3a**	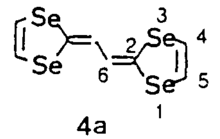 **4a**
5.88 (s, 2 H, H_6)	5.84 (d, 2 H, J = 3 Hz, H_7)	5.64 (d, 1 H, J = 11 Hz, H_6)	6.10 (s, 2 H, H_6)
	6.08 (d, 2 H, J = 3 Hz, H_6)	6.29 (d, 1 H, J = 11 Hz, $H_{6'}$)	
6.23 (s, 4 H, $H_{4,5}$)	6.21 (s, 2 H, H_4 or H_5)	6.19 (s, 2 H, $H_{4,5}$)	7.08 (s, 4 H, $H_{4,5}$)
	6.22 (s, 2 H, H_4 or H_5)	7.07 (s, 2 H, $H_{4',5'}$)	

^{a} Measured in $CDCl_3$.

Scheme IV

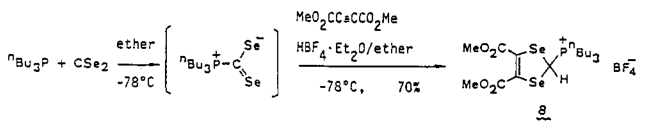

1i) were obtained in yields of 83, 77, and 86%, respectively.

The synthesis of **3a** and **4a** was accomplished by the same method as above, except for the use of (4,5-dicarbomethoxy-1,3-diselenol-2-yl)tri-*n*-butylphosphonium tetrafluoroborate (**8**) in place of the sulfur analogue **5b**.[23] The salt **8** was prepared in a good yield (ca. 70%) by the reaction of the tri-*n*-butylphosphine–carbon diselenide adduct with dimethyl acetylenedicarboxylate and by subsequent treatment with fluoroboric acid etherate (Scheme IV). The phosphorane generated in situ from **8** and Et_3N in THF was reacted with 2 equiv of glyoxal at room temperature to provide the aldehyde **9** in 84% yield (see Table I). The Wittig reactions of **9** with **8** and **5b** afforded the tetraester derivatives of **3a** and **4a** (**3b** and **4b**) in yields of 60 and 94%, respectively (see Table II). Their demethoxycarbonylation with $LiBr \cdot H_2O$ in hot HMPA gave the unsubstituted compounds **3a** and **4a** in yields of 68 and 61%, respectively.

In principle, there are two possible conformations, transoid and cisoid, for **1**, **3**, and **4**, but the latter conformation is anticipated to be unfavorable because of steric repulsion between two heterocycles. Although the olefinic proton NMR signals of the unsymmetrical derivatives **1f**, **1g**, **1i**, and **1j** appeared as a singlet, **1h**, **4a**, and **4b** showed two different olefinic proton signals as two doublets. Judging from the coupling constants (11 Hz), **1h**, **4a**, and **4b** are concluded to have the transoid conformation. Therefore, all the ethanediylidene derivatives are assumed to have transoid conformations.

Synthesis of 1,4-But-2-enediylidene-2,2′-bis(1,3-dithiole)s (2). The tetraester derivatives of **2a** and its 2,2′-diphenyl-substituted compound (**2b** and **2f**) synthesized by Mckinnon et al.[12] and 2-cyclohexene-1,4-diylidene-2,2′-bis(4,5-bis(methoxycarbonyl)-1,3-dithiole) synthesized by Cava et al.[13b] were treated with $LiBr \cdot H_2O$ in hot HMPA,[21] and the demethoxycarbonylated **2a**, **2g**, and **2i** were obtained in moderate yields of 31, 45, and 68%, respectively. However, this method was unsuccessful for the synthesis of tetramethyl-**2c**, tetraphenyl-**2d**, and dibenzo-**2e** derivatives of **2a**. Therefore, a new synthetic method was developed that involves the reductive coupling of 2-(formylmethylene)-1,3-dithioles **7a**, **7c**, **7d**, and **7e** with a $TiCl_4$–$LiAlH_4$ complex in the presence of $(n\text{-}Bu)_3N$ in THF.[24] With this method the above compounds were successfully synthesized in yields of 52–100%. However, when **7b** was used in this reaction, the expected product **2b** was not obtained at all.

To determine the configuration about the central C=C bond of **2a**, its ^1H NMR and electronic spectra were compared with those of **2g** and **2i**, which have rigid trans and cis configurations, respectively. However, no significant difference was observed in the spectral comparison. Fortunately, there was an observed definitive difference in the *g* values of the cation radicals, which were generated by the electrochemical one-electron oxidation and measured by ESR spectroscopy. Thus, the *g* value of $2a^{\bullet+}$, 2.0072, was equivalent to that of $2g^{\bullet+}$. On the other hand, $2i^{\bullet+}$ had a smaller value (2.0068). If it can be assumed that the configuration of **2** does not change largely in the

---

(23) For the previous communication; Yoshida, Z.; Awaji, H.; Sugimoto, T. *Tetrahedron Lett.* **1984**, 4227.

(24) Ishida, A.; Mukaiyama, T. *Chem. Lett.* **1976**, 1127.

neutral and cation radical states, it is reasonably inferred that **2a** and the other derivatives have trans configurations.

^{1}H and ^{13}C NMR Spectra. The ^{1}H NMR spectra of the representative new donors **1a**, **2a**, **3a**, and **4a** were measured in $CDCl_3$ (see Table III). In the case of the 1,3-dithiole ring protons the signals appear at almost the same field (δ 6.19–6.23), and the chemical shifts are smaller by 0.09–0.13 ppm than the value for TTF (δ 6.32). On the other hand, the 1,3-diselenole ring protons appear at a higher field than those of the 1,3-dithiole ring, and there is no change in the chemical shifts for **3a** and **4a**. However, an unexpected observation with respect to chemical shift of the olefinic protons was obtained. Thus, the signals of olefinic protons are observed at δ 5.88 for **1a** and at δ 6.10 for **3a**. For **4a**, two different signals appeared at δ 5.64 and 6.29, and from the comparison with **1a** and **3a** the higher field signal can be easily assigned to the H-6′ proton, with the lower field signal to the H-6 proton. The H-6′ proton is shifted by 0.2 ppm to higher field, while the H-6 proton is shifted by 0.2 ppm to lower field, respectively, as compared with the corresponding protons of **4a** and **1a**. We assume that this abnormal shift is due to the change in the electron density distribution produced by the electron flow from the 1,3-dithiole to the 1,3-diselenole ring as discussed in the following ^{13}C NMR analysis, in addition to the different anisotropic effects between S and Se atoms.

The ^{13}C NMR spectra were also measured for the new donors and TTF for comparison. The chemical shifts and their assignment to each carbon atom are shown in Figure 1. The definitive assignment to the ring (C-4, -5) and olefinic carbons (C-6, -7) was made on the basis of the $J_{^{13}C-H}$ coupling constant values (184–185 Hz for C-4, -5, 149–157 Hz for C-6, -7) and on the appearance of two-bond coupling with the ring hydrogen atom ($^2J_{^{13}C-H}$ = 5–6 Hz for C-4, -5, -5′, -6′). The two signals at δ 113.2 ($J_{^{13}C-H}$ = 156 Hz) and 125.0 (149 Hz) of **2a** were assigned to the C-7 and -6 carbons, respectively, since the inner sp^2 carbons of **2i** appear at δ 118.5 (158 Hz).

When the ^{13}C chemical shifts are compared between TTF and **1a**, the C-4 and C-5 carbons (δ 117.1, 117.7) of the latter compound are shifted to a slightly higher field than are those of the former (δ 119.0). However, such a change in the shifts is not observed between **1a** and **2a**. On the other hand, the C-2 carbon shows a downfield shift by about 22 and 3 ppm, respectively, in going from TTF to **1a** and to **2a**. These results suggest some contribution of the polar structures as shown in Scheme V to the ground state of **1a** and **2a**. A similar argument has also been made for a series of 1,4-dithiafulvenes.[25] On the other hand, such a polarization is not expected for TTF. The difference of electronic structures between **1a**, **3a**, and **4a** can be shown from comparison of their ^{13}C NMR spectra. The C-4 (and -5) and -6 carbons of **3a** revealed a downfield shift by about 3 and 10 ppm, respectively, as compared with the corresponding carbons of **1a**. However, the C-2 carbon signal of **3a** is reversely shifted to higher field by about 7 ppm relative to **1a**. This change might be due to a decreased contribution of the polar structure to the ground state of **3a** as compared with that of **1a** (see Scheme V). As for **4a**, the C-4, -5, -4′, and -5′ carbons appear at a field similar to the corresponding carbons of **3a** and **1a**. However, the C-2′ carbon shifts upfield by about 2 ppm relative to that of **3a**, while the C-2 carbon signal is observed at a lower field (by about 2 ppm) than that of **1a**. This unusual shift suggests a more significant contribution of the polar structure (B), rather than the reverse polar

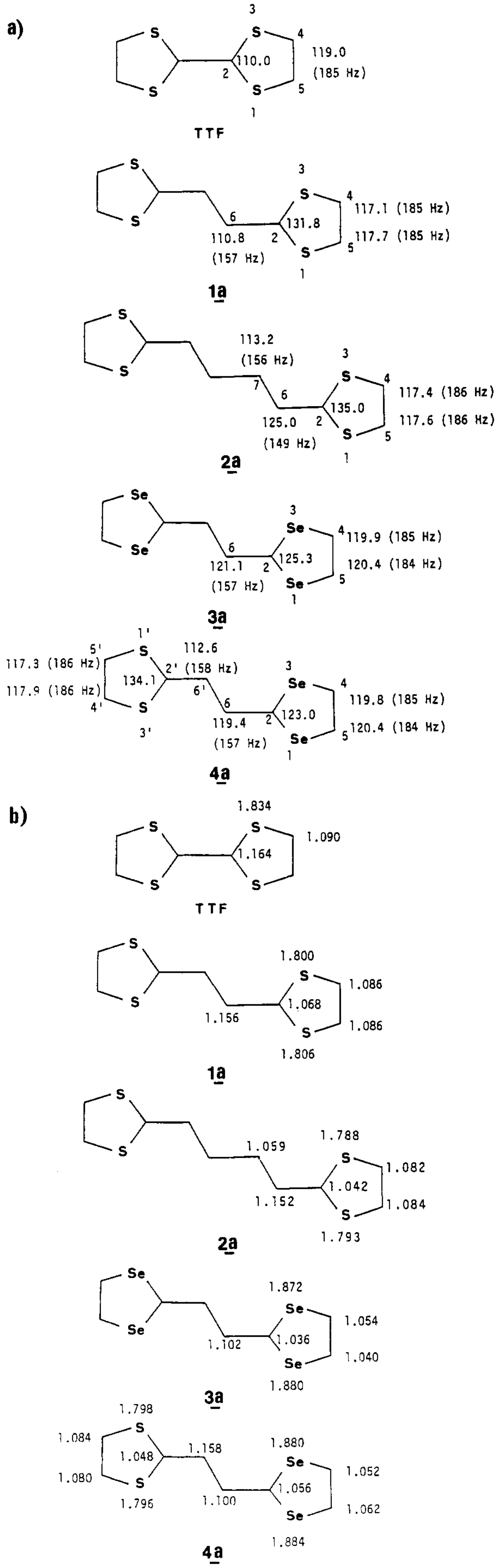

Figure 1. (a) ^{13}C NMR chemical shifts in $CDCl_3$ and (b) the π-electron density distributions of TTF, **1a**, **2a**, **3a**, and **4a**.

---

[25] Lakshmikantham, M. V.; Cava, M. P. *J. Org. Chem.* **1981**, *46*, 3246.

Scheme V

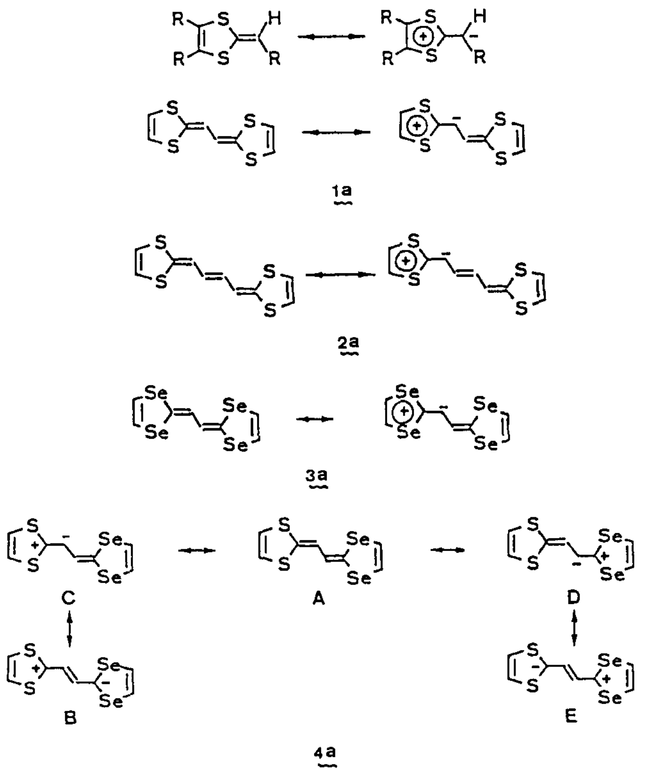

structure (E), in addition to the covalent structure (A, see Scheme V).

The π-electron density distributions of the new donors and also TTF are calculated by the PPP type SCF method,[14] and the results are compared with the ^{13}C chemical shifts (see Figure 1). As is obvious from this figure, the central sp^2 carbon atoms of TTF are negatively charged. The negative charge borne by the central butadiene type group of **1a** is larger than that borne by the central ethylene type group in TTF. A similar situation is also seen in the case of **2a**. The negative charge on the central 1,3,5-hexatriene group is comparable to that of **1a** or slightly larger. In going from TTF to TSF the negative charge on the central C=C double bond is slightly decreased. This is also the case for the other pairs discussed in this paper. The replacement of sulfur atoms in these compounds by selenium atoms does not cause a drastic change in the situation concerning the electron flow in the molecules just as for the case of the orbital energies. The estimated charge flows from the two terminal five-membered rings to the central olefinic carbons of these compounds are as follows: **1a**, −0.312*e*; **2a**, −0.422*e*; **3a**, −0.204*e*; **4a**, −0.258*e*. These values could provide a measure of the contribution of the polar structure: **1a**, 16%; **2a**, 21%; **3a**, 10%; **4a**, 13%.

Electronic Spectra. Electronic spectra of TTF and **1a**–**4a** measured in chloroform are shown in Figures 2 and 3. As is seen in Figure 2, the band shapes of **1a** and **2a** are very similar to each other but quite different from that of TTF in the low-energy region. The compound **1a** shows two strong absorption bands at 404 and 384 nm, while for **2a** two absorption bands were observed at about 30 nm longer wavelength than **1a** (432 and 409 nm). On the other hand, the selenium analogues **3a** and **4a** show absorptions in a range similar to that of **1a** (see Figure 3), but only one broad strong absorption band appears in those cases at around 378 and 388 nm, respectively.

To understand the origin of the absorption band exhibited by the new donors, their electronic transitions were calculated by using the PPP type SCF method with configuration interactions (CI).[14] The observed electronic spectral band characteristics with the calculated singlet–singlet (s–s) electronic transitions are summarized in Table IV. Also, the HO-π-MOs and LU-π-MOs are schematically drawn in Figure 4.

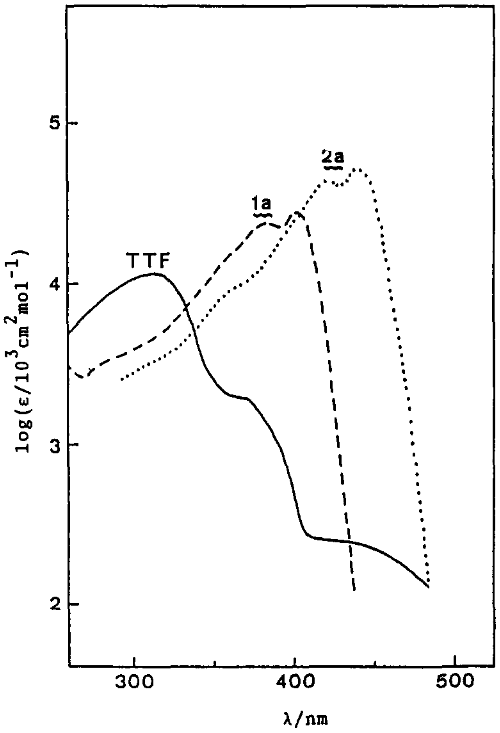

Figure 2. Electronic spectra of TTF, **1a**, and **2a** in $CHCl_3$.

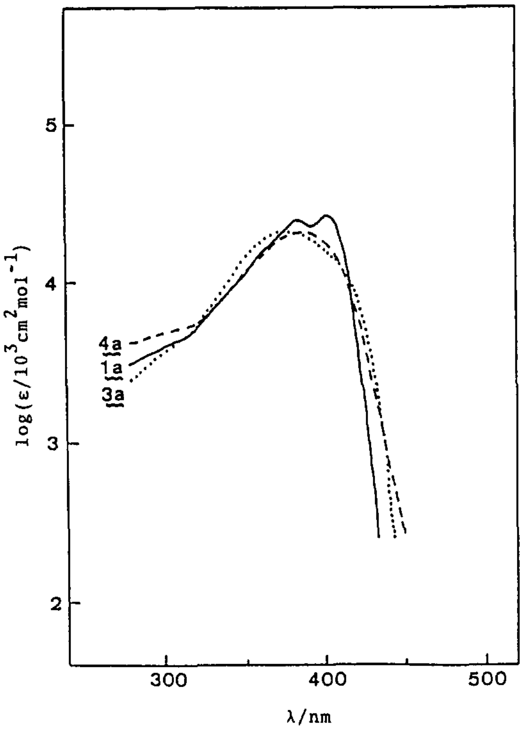

Figure 3. Electronic spectra of **1a**, **3a**, and **4a** in $CHCl_3$.

There has been a controversy regarding the assignment of the electronic transitions of TTF. Coffen et al.[26] in-

---

[26] Coffen, D. L.; Chambers, J. Q.; Williams, D. R.; Garrett, P. E.; Canfield, N. D. *J. Am. Chem. Soc.* **1971**, *93*, 2258.

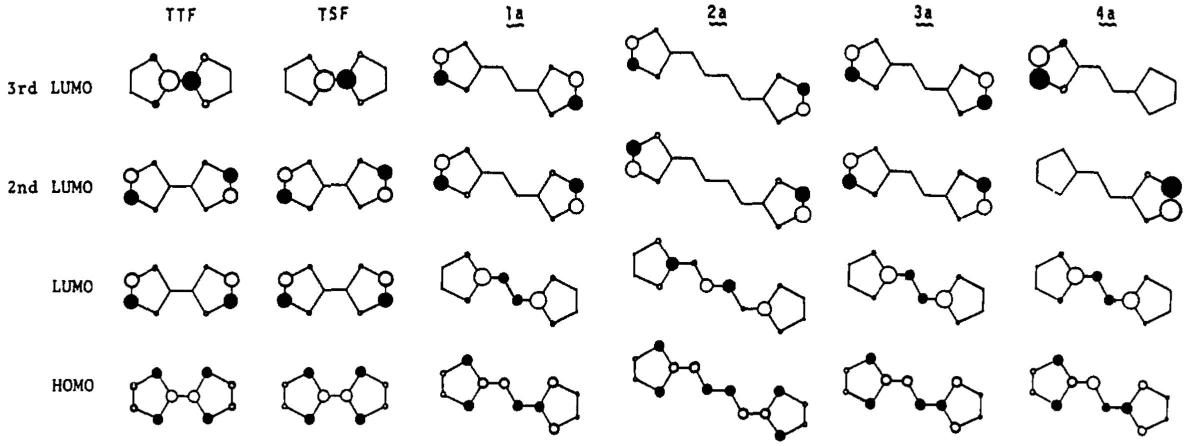

Figure 4. Schematic representations of highest occupied (HOMO), lowest unoccupied (LUMO), the second lowest unoccupied (second LUMO), and the third lowest unoccupied (third LUMO) MOs of TTF, TSF, **1a**, **2a**, **3a**, and **4a**, calculated by the PPP type SCF method. The areas of the circles are proportional to the squares of the LCAO coefficients. The blank and filled circles symbolize positive and negative signs of these coefficients, respectively.

terpreted the first three bands as the $^1B_{1u}$ $\sigma^* \leftarrow \pi$, $^1B_{2g}$ $\sigma^* \leftarrow \pi$, and $^1B_{3u}$ $\pi^* \leftarrow \pi$ transitions based on an extended Hückel calculation. However, Zahradník et al.[27] used the PPP type SCF-CI calculation and assigned the first band to that due to the $^1B_{1g}$ $\pi^* \leftarrow n$ transition and the following two bands to the $^1B_{3u}$ and $^1B_{2u}$ $\pi^* \leftarrow \pi$ transitions. Recently, Gleiter et al.[28] assigned the first three bands as $^1B_{1g}$, $^1B_{3g}$, and $^1B_{2u}$ $\pi^* \leftarrow \pi$ transitions, respectively, on the basis of the measurement of the polarized electronic spectrum in stretched polyethylene film and on the results of the PPP type MO calculation. Now there appear to be no ambiguities about the assignments of the second and third bands at 3.37 and 3.87 eV, respectively. The 3.37-eV band is associated with the transition mainly arising from the LU-π-MO ← HO-π-MO excitation, namely, with the transition from the π-orbital localized in the central tetrathioethylene grouping ($S_2C{=}CS_2$) to the π*-orbital localized on the two terminal ethylenes. This means that the polarization occurs along the short molecular axis. The 3.87-eV band is due to the third LU-π-MO ← HO-π-MO transition polarized along the long molecular axis, accompanied by slight electron migration from the sulfur atoms to the central ethylenic group.

On the other hand, the character of electronic transitions of **1a** is quite different from that of TTF. The longest wavelength band at 3.07 eV is very strong, which from the PPP CI calculation is due to the ^1B_u LU-π-MO ← HO-π-MO transition polarized along the long molecular axis and accompanied by slight electron migration from the sulfur atoms to the central butadiene type group, as in the case of the 3.87-eV band of TTF. The band at 3.23 eV is assigned to the second LU-π-MO ← HO-π-MO transition polarized along the short molecular axis. A very similar situation was also obtained for **2a**. Thus, the first strong band at 2.87 eV is due to the ^1B_u LU-π-MO ← HO-π-MO transition polarized along the long molecular axis and accompanied by slight electron migration from the sulfur atoms to the central hexatriene group. The following band at 2.99 eV is associated with the second LU-π-MO ← HO-π-MO transition polarized along the short molecular axis. The absorption bands associated with the LU-π-MO ← HO-π-MO transition are shifted to longer wavelength with lengthening of the π-systems, TTF < **1a** < **2a**.[29] This observation is in agreement with the result obtained from the calculations.

Scheme VI

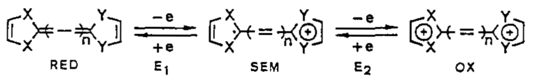

The electronic spectrum of TSF was measured by Engler and Patel.[30] According to their data there is no drastic change between TSF and TTF in the lower electronic transitions. In fact, the present PPP CI calculations demonstrate the similarity in character between the lower electronic transitions for both of these compounds. The second band at 3.40 eV, which is quite close to the position of the 3.37-eV band of TTF, can be ascribed to the $^1B_{3u}$ LU-π-MO ← HO-π-MO transition polarized along the short molecular axis. The strong band at 4.13 eV is due to the $^1B_{2u}$ third LU-π-MO ← HO-π-MO transition polarized along the long molecular axis and is, again, close to the 3.87-eV band of TTF. The same situation is also seen in the case of the **3a** and **1a** pair. Thus, the strong and broad band of **3a** at around 3.28 eV can be mainly assigned as the ^1B_u LU-π-MO ← HO-π-MO transition polarized along the long molecular axis, and the ^1B_u second LU-π-MO ← HO-π-MO transition polarized along the short molecular axis, in part, participates. The principal character of electronic transitions in lower energy remains the same even in the case of **4a**. The strong and broad band of **4a** at ca. 3.20 eV corresponds to the $^1A'$ LU-π-MO ← HO-π-MO transition polarized along the long molecular axis. The 4.01- and 4.20-eV transitions also are included as components of the observed 3.20-eV band. In addition, it should be noted that the lowest electronic transitions are shifted to higher energy in the order **1a** < **4a** < **3a** with increasing replacement of sulfur atoms in 1,3-dithiole rings by selenium atoms. This trend has been well reproduced by the PPP CI calculations as seen in Table IV.

Electrochemical Properties. The redox processes and potentials of the newly synthesized 1,3-dichalcogenolidene systems were examined by use of cyclic voltammetry. The representative cyclic voltammograms of the parent systems **1a**, **2a**, **3a**, and **4a** are shown in Figure 5 together with that

---

[27] Zahradník, R.; Cársky, P.; Hünig, S.; Kiesslich, G.; Schentzow, D. *Int. J. Sulfur Chem., Part C* **1971**, *6*, 109.

[28] Gleiter, R.; Schmidt, E.; Cowan, D. O.; Ferraris, J. P. *J. Electron Spectrosc. Relat. Phenom.* **1973**, *2*, 207.

[29] The similar tendency was also observed in related systems of tetrathiaethylene and 1,1,4,4-tetrathiabutadiene: Sandman, D. J.; Zoski, G. D.; Burke, W. A.; Hamill, G. P.; Caesar, G. P.; Baker, A. D. *J. Chem. Soc., Chem. Commun.* **1981**, 829.

[30] Engler, E. M.; Patel, V. V. *J. Am. Chem. Soc.* **1974**, *96*, 7376.

Table IV. Calculated and Observed Electronic Transitions for TTF, TSF, 1a, 2a, 3a, and 4a

	calcd					obsd		
	sym	Ee^{s-s}, eV	f	CI composition[b]		λ_{max}, nm	Ee, nm	$10^{-3}\epsilon$, cm^2/mol
TTF[c]	B_{1g}	3.60	0.0	$9 \leftarrow 7$	0.989	444	2.79	172
	B_{3u}	3.64	0.189	$8 \leftarrow 7$	0.988	368	3.37	1893
	B_{2u}	4.16	0.610	$10 \leftarrow 7$	0.998	320	3.87	11400
	A_g	5.98	0.0	$10 \leftarrow 6$	0.919	311	3.99	11400
	B_{1g}	6.01	0.0	$8 \leftarrow 6$	0.925			
	B_{3u}	6.06	0.298	$9 \leftarrow 6$	0.905			
				$10 \leftarrow 5$	−0.361			
	B_{2u}	6.20	0.416	$8 \leftarrow 5$	0.717			
				$9 \leftarrow 4$	−0.693			
TSF[d]	B_{1g}	4.30	0.0	$9 \leftarrow 7$	0.981	495	2.50	132
	B_{3u}	4.34	0.224	$8 \leftarrow 7$	0.982	365	3.40	1413
	B_{2u}	4.62	0.545	$10 \leftarrow 7$	0.998	300	4.13	12300
	A_g	6.07	0.0	$10 \leftarrow 6$	0.973	287	4.32	12000
	B_{1g}	6.28	0.0	$8 \leftarrow 6$	0.908			
				$9 \leftarrow 3$	−0.260			
				$10 \leftarrow 4$	−0.289			
	B_{3u}	6.31	0.278	$8 \leftarrow 3$	−0.250			
				$9 \leftarrow 6$	0.888			
				$10 \leftarrow 5$	0.358			
1a	B_u	3.34	1.134	$9 \leftarrow 8$	0.994	404	3.07	26500
	A_g	3.83	0.0	$11 \leftarrow 8$	0.966			
	B_u	3.84	0.196	$10 \leftarrow 8$	0.966	384	3.23	24700
	A_g	4.76	0.0	$9 \leftarrow 7$	0.978			
	A_g	5.38	0.0	$12 \leftarrow 8$	0.987			
	A_g	5.76	0.0	$10 \leftarrow 7$	0.741			
				$9 \leftarrow 5$	0.553			
	B_u	5.76	0.025	$11 \leftarrow 7$	0.734			
				$9 \leftarrow 6$	−0.559			
	B_u	6.16	0.398	$11 \leftarrow 5$	−0.641			
				$10 \leftarrow 6$	0.639			
				$9 \leftarrow 4$	−0.395			
2a	B_u	2.84	1.612	$10 \leftarrow 9$	0.984	432	2.87	53100
	A_g	3.90	0.0	$11 \leftarrow 8$	0.345			
				$12 \leftarrow 9$	0.921			
	B_u	3.91	0.169	$11 \leftarrow 9$	0.922	409	2.99	43400
				$12 \leftarrow 8$	0.342			
	A_g	4.00	0.0	$10 \leftarrow 8$	0.955			
	A_g	4.64	0.0	$10 \leftarrow 8$	0.209			
				$13 \leftarrow 9$	0.955			
	B_u	5.51	0.127	$10 \leftarrow 6$	0.274			
				$10 \leftarrow 7$	0.760			
				$14 \leftarrow 9$	−0.456			
	A_g	5.57	0.0	$10 \leftarrow 5$	0.665			
				$11 \leftarrow 8$	0.547			
				$12 \leftarrow 7$	0.296			
				$12 \leftarrow 9$	−0.306			
				$13 \leftarrow 6$	0.236			
	B_u	5.58	0.014	$10 \leftarrow 7$	−0.285			
				$10 \leftarrow 6$	0.606			
				$11 \leftarrow 7$	0.286			
				$11 \leftarrow 9$	−0.288			
				$12 \leftarrow 8$	0.526			
				$13 \leftarrow 5$	0.215			
	B_u	5.80	0.022	$10 \leftarrow 3$	0.210			
				$10 \leftarrow 7$	0.370			
				$13 \leftarrow 8$	0.385			
				$14 \leftarrow 9$	0.763			
	A_g	5.98	0.0	$10 \leftarrow 5$	0.653			
				$11 \leftarrow 8$	−0.676			
	B_u	5.99	0.607	$10 \leftarrow 6$	0.641			
				$12 \leftarrow 8$	−0.667			
	A_g	6.21	0.0	$10 \leftarrow 4$	−0.353			
				$11 \leftarrow 5$	0.650			
				$12 \leftarrow 6$	0.649			
3a	B_u	3.64	1.043	$9 \leftarrow 8$	0.993	378	3.28	20400
	A_g	4.41	0.0	$10 \leftarrow 7$	0.285			
				$11 \leftarrow 8$	0.954			
	B_u	4.42	0.223	$10 \leftarrow 8$	0.955			
				$11 \leftarrow 7$	0.278			
	A_g	4.85	0	$9 \leftarrow 7$	0.988			
	A_g	5.79	0	$12 \leftarrow 8$	0.983			
	B_u	5.92	0.037	$9 \leftarrow 5$	0.856			
				$10 \leftarrow 6$	0.204			
				$11 \leftarrow 7$	−0.381			
	A_g	5.92	0.0	$9 \leftarrow 4$	0.856			
				$10 \leftarrow 7$	0.368			

Table IV (Continued)

	calcd					obsd		
	sym	Ee^{s-s}, eV	*f*	CI composition[b]		λ_{max}, nm	Ee, nm	$10^{-3}\epsilon$, cm^2/mol
	B_u	6.24	0.297	9 ← 6	0.826			
				10 ← 5	−0.374			
				11 ← 4	0.374			
4a	A′	3.48	1.085	9 ← 8	0.993	388	3.20	20300
	A′	4.01	0.105	11 ← 8	0.966			
				11 ← 7	0.220			
	A′	4.20	0.095	10 ← 7	−0.274			
				10 ← 8	0.958			
	A′	4.85	0.008	9 ← 7	0.983			
	A′	5.57	0.0003	12 ← 8	0.989			
	A′	5.85	0.015	9 ← 5	0.647			
				9 ← 6	−0.444			
				11 ← 6	−0.213			
				11 ← 7	−0.486			
				11 ← 8	0.217			
	A′	5.89	0.040	9 ← 4	0.538			
				10 ← 6	−0.210			
				10 ← 7	0.748			
				10 ← 8	0.242			
	A′	6.191	0.320	9 ← 5	0.269			
				9 ← 6	0.401			
				10 ← 4	0.211			
				11 ← 5	0.688			
				11 ← 6	−0.460			

[a] Solvent: $CHCl_3$. [b] The transition indicated as *j* ← *i* refers to a one-electron excitation from the valence π orbital *i* to *j*. The second column gives the CI coefficient of the configuration *j* ← *i*. [c] Electronic spectral data were taken from ref 27.

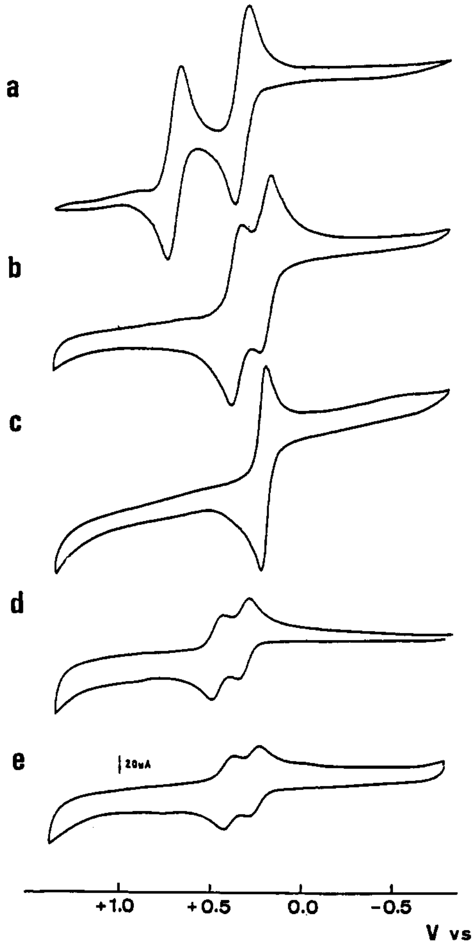

Figure 5. Cyclic voltammograms of (a) TTF, (b) **1a**, (c) **2a**, (d) **3a**, and (e) **4a** in CH_3CN containing 0.1 M Et_4NClO_4 at room temperature (scan rate 43 mV/s).

of TTF for comparison. Like TTF, the other systems, except for **2a**, exhibit two pairs of waves and each pair is electrochemically reversible. For both waves the voltage difference between anodic and cathodic peaks is about 60 mV,[31] indicating two-step one-electron transfer. On the other hand, **2a** shows only one pair of waves with a peak separation of about 30 mV.[31] This redox process is reversible and involves transfer of two electrons in one step. It is conceivable that the two steps are due to electron loss and gain between the neutral and radical cation states and between the radical cation and dication states, respectively (see Scheme VI). In fact the radical cations and dications were synthesized by chemical oxidation and characterized. Thus, treatment of **1a** and **1c** with 0.5 equiv of bromine gave quantitatively the corresponding cation radical salts $\mathbf{1a}^{\bullet+}Br^-$ and $\mathbf{1c}^{\bullet+}Br^-$, respectively, as purple solids. The addition of an equimolar amount of bromine quantitatively afforded the corresponding dication salts $\mathbf{1a}^{2+}2Br^-$, $\mathbf{1c}^{2+}2Br^-$, and $\mathbf{2c}^{2+}2Br^-$, respectively (see Scheme VII). On the other hand, no formation of radical cation and dication salts was observed in the reaction of **1b** with bromine. Instead, the dibromo-substituted product was obtained in almost quantitative yield.[32] In this case the radical cation and dication of **1b** ($\mathbf{1b}^{\bullet+}$ and $\mathbf{1b}^{2+}$) are so reactive as to

Scheme VII

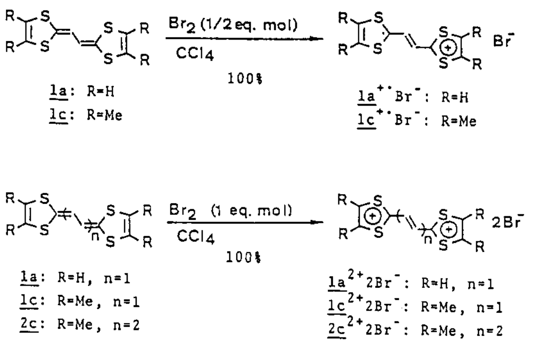

---

(31) In the case of a reversible single-step electron transfer, the voltage separation between anodic and cathodic peaks is theoretically given by 60/*n* (mV), where *n* denotes the number of electrons involved in the redox process: Bard, A. J.; Faulkner, L. R. *Electrochemical Methods: Fundamentals and Applications*; Wiley: New York, 1980; Chapter 6.

(32) Sugimoto, T.; Awaji, H.; Misaki, Y.; Yoshida, Z.; Kai, Y.; Nakagawa, H.; Kasai, N. *J. Am. Chem. Soc.* **1985**, *107*, 5792.

Table V. Redox Potentials E_1 and E_2 and K_{SEM} Values of 1–4

donor	E_1[b]	E_m[a,b]	E_2[b]	$E_2 - E_1$	K_{SEM}[c]
1a	0.20		0.36	0.16	5.2×10^2
1b	0.60		0.74	0.14	2.4×10^2
1c	0.19		0.34	0.15	3.5×10^2
1d	0.28		0.46	0.18	1.1×10^3
1e	0.47		0.64	0.17	7.6×10^2
1f	0.49		0.64	0.15	3.5×10^2
1g	0.37		0.53	0.16	5.2×10^2
1h	0.38		0.59	0.21	3.6×10^3
1i	0.23		0.39	0.16	5.2×10^2
1j	0.33		0.50	0.17	7.6×10^2
2a	0.217	0.22	0.223	0.006	1
2b	0.542	0.55	0.553	0.006	1
2c	0.207	0.21	0.213	0.006	1
2d	0.317	0.32	0.323	0.006	1
2e	0.467	0.47	0.473	0.006	1
2f	0.597	0.60	0.603	0.006	1
2g	0.277	0.28	0.283	0.006	1
2h	0.567	0.57	0.573	0.006	1
2i	0.227	0.23	0.233	0.006	1
3a	0.33		0.47	0.14	2.4×10^2
3b	0.64		0.81	0.17	7.6×10^2
4a	0.26		0.40	0.14	2.4×10^2
4b	0.62		0.77	0.15	3.5×10^2
TTF[d]	0.34		0.71	0.37	1.9×10^6
TMTTF[d]	0.25		0.61	0.36	1.3×10^6
DBTTF[d]	0.61		0.93	0.32	2.7×10^5

[a] $E_m = (E_1 + E_2)/2$. [b] V vs Ag/AgCl, measured in CH_3CN containing 0.1 M Et_4NClO_4 by using platinum working and counter electrodes with a scan rate of 43 mV/s. [c] $E_2 - E_1 = 0.0591 \times \log K_{SEM}$, $K_{SEM} = [SEM]^2/[RED][OX]$. [d] Under the same condition were measured the redox potentials of TTF, tetramethyl-TTF (TMTTF), and dibenzo-TTF (DBTTF).

Table VI. Physical Properties of the Charge-Transfer Salts of New Donors and TTF with TCNQ and DMTCNQ

donor	acceptor	D:A	$\tilde{\nu}_{C\equiv N}$, cm^{-1}	σ_{RT}, S/cm	E_a, eV
1a	TCNQ	1:1	2187	0.79[a]	0.09–0.4
1a	DMTCNQ	1:1	2188	0.0711[a]	0.055–0.086
1c	TCNQ	1:1	2175	3.7×10^{-8}[b]	0.48
1c	DMTCNQ	1:0.72	2192	4×10^{-6}[b]	
1i	TCNQ	1:1	2185	0.058[a]	0.083
1i	DMTCNQ	1:1	2180	1×10^{-5}[b]	
2i	TCNQ	1:1	2188	0.26[a]	0.062
2i	DMTCNQ	1:1	2188	3×10^{-4}[b]	
3a	TCNQ	2:3	2196	0.24[a]	0.038
3a	DMTCNQ	1:1	2206	6×10^{-12}[b]	
4a	TCNQ	2:3	2194	0.072[a]	0.046
4a	DMTCNQ	1:1	2200	1×10^{-6}[b]	
TTF	TCNQ	1:1	2201	2.5[a]	

[a] Measured by using the four-probe method. [b] Measured by using the two-probe method.

undergo a nucleophlic attack of Br^-.

The first (E_1) and second (E_2) redox potentials were measured and are summarized in Table V. For **4** the two overlapping redox potentials were separated into the E_1 and E_2 values according to the Myers and Shain analysis.[33] As is obvious from the table, the E_1 value of **1** is more negative by 0.06–0.14 V and the E_2 value is more negative by 0.25–0.29 V than those of corresponding TTF derivatives. Such a decreasing E_1 value implies that **1** has a higher electron-donating ability than TTF. In addition, the remarkable decrease in the E_2 value suggests better stabilization of the dication state of **1** as compared with that of TTF. The increased stabilization of the dication state with increasing chain length can be understood by an increase of distance between the two positive charges. As for **2**, unexpectedly the E_1 value is almost equal to that of **1**, but a marked decrease is observed for the E_2 value. A plausible explanation is that there is less effective π-conjugation between the two 1,3-dithiole systems as a result of the presence of two C–C single bonds in the neutral state; however, this conjugation becomes more effective in the cation radical because the C–C bond rotation is restricted. From comparison of the E_1 values of **1**, **3**, and **4**, the donating ability tends to become weaker by substituting selenium atoms for sulfur atoms in 1,3-dithiole rings, i.e., the E_1 values move toward more positive values in the order **1** < **4** < **3**. As expected, a substituent effect on the oxidation potentials of **1**, **2**, **3**, and **4** was observed; the substitution of electron-donating groups at the 4- and 5-positions of 1,3-dithiole ring decreased the oxidation potentials, while by introducing electron-withdrawing groups the oxidation becomes more difficult.

It is noteworthy that the ($E_2 - E_1$) values of the new systems are considerably smaller than those of TTFs. In particular, **2** has a very small value (6 mV). The ($E_2 - E_1$) can be related to the semiquinone formation constant $K_{SEM} = [SEM]^2/([RED][OX])$, which represents the thermodynamic stability of cation radicals in the SEM stage, by the equation $E_2 - E_1 = 0.059 \log K_{SEM}$ (V, 25 °C).[34] In Table V the K_{SEM} values of **1**, **2**, **3**, and **4** are also included. The values for TTF are on the order of 10^6, while **1**, **3**, and **4** have smaller values of 10^2–10^3. The value for **2** is remarkably small (ca. 1). Therefore, the thermodynamic stabilities of cation radicals decrease in the order TTF > **1** $\simeq$ **3** $\simeq$ **4** > **2**. This implies that the cation radicals tend to disproportionate in the reverse order.

CT Complexes of the New 1,3-Dichalcogenolidene Systems with TCNQ and DMTCNQ. The formation of CT complexes of the new 1,3-dichalcogenolidene donor systems with TCNQ was studied first. The TCNQ complex formation was carried out by mixing acetonitrile solutions of the donor and TCNQ in an equimolar amount. The donors **1a**, **1b**, and **1c** provided fine dark purple crystals that had compositions of D:A = 1:1.[35] Also, the complexes of **3a** and **4a** were obtained as fine crystals whose composition was D:A = 2:3.[35] For comparison, the TTF–TCNQ complex was prepared in a manner similar to that given above. Complex formation with **2a** and **2b** was evidenced by a change in the color of the solution to purple immediately after mixing the donor and acceptor. However, the color disappeared gradually, thus suggesting the decomposition of the complexes. This suggests a thermodynamic instability of the complexes, perhaps arising from energetically unfavorable free rotation around the central olefinic bond. In fact, using the same butene-1,4-diylidene derivative with a rigid triene structure, **2c**, a stable 1:1 TCNQ complex was isolated as fine dark green needles.

The electric conductivities of **1a**–TCNQ, **1b**–TCNQ, **1c**–TCNQ, **2c**–TCNQ, $(\mathbf{3a})_2$–$(TCNQ)_3$, $(\mathbf{4a})_2$–$(TCNQ)_3$, and TTF–TCNQ as a reference were measured on the compressed pellets. Table VI shows the room-temperature electric conductivities (σ_{RT}, S/cm) and activation energies (E_a, eV) of the TCNQ complexes and also the nitrile stretching absorption bands ($\tilde{\nu}_{C\equiv N}$, cm^{-1}) in the IR spectra. Except for the **1c**–TCNQ complex, the other TCNQ complexes exhibited comparatively high electric conductivities (5×10^{-2}–8×10^{-1} S/cm). Among them the highest electric conductivity was observed for the **1a**–TCNQ complex, and the value was ca. one-third that of the TTF–TCNQ com-

---

[33] Myers, R. L.; Shain, I. *Anal. Chem.* **1969**, *41*, 980.

[34] (a) Deuchert, K.; Hünig, S. *Angew. Chem., Int. Ed. Engl.* **1978**, *17*, 875. (b) Hünig, S.; Berneth, H. *Top. Curr. Chem.* **1980**, *92*, 1.

[35] The compositions of D:A in the CT complexes were unchangeable even with excess TCNQ and donor.

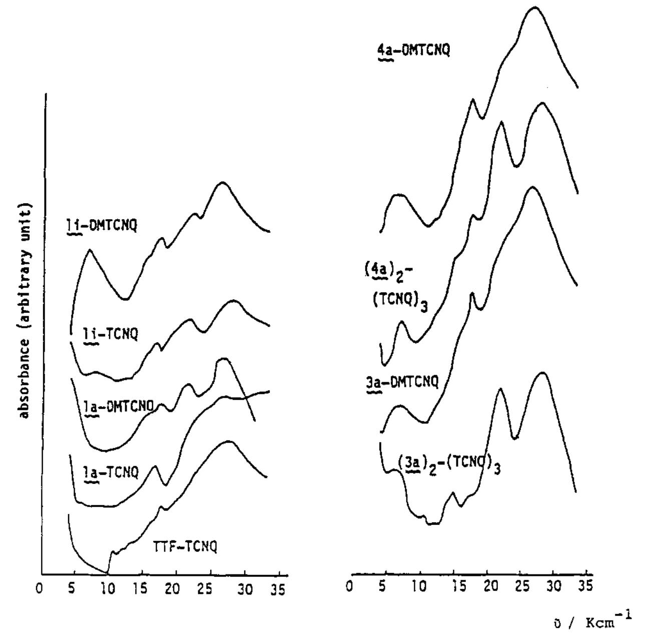

Figure 6. Powder absorption spectra in KBr pellets.

plex, measured under the same conditions. When a comparison was made between the E_1 values of the donors and $\tilde{\nu}_{C\equiv N}$ values of the TCNQ complexes, it was found that the $\tilde{\nu}_{C\equiv N}$ shifts to lower wavenumber with a decrease in the E_1 value. This means that the degree of electron transfer from the donor to TCNQ increases in the TCNQ complex, as the E_1 value of the donor becomes smaller. Now, DMTCNQ, a weaker acceptor than TCNQ, was next used for complex formation with the new donors. The electric properties of the DMTCNQ complexes are also shown in Table VI. The DMTCNQ complexes showed decreased electric conductivities by 10–10^{11} S/cm as compared with the corresponding TCNQ complexes. For the TCNQ complexes with comparatively higher electric conductivities the E_a values were small (0.03–0.09 eV). On the other hand, the insulating salts such as **1c**–TCNQ had considerably higher activation energies (0.48 eV for **1c**–TCNQ). These results are consistent with those of the electronic spectra of the complexes in KBr pellets.[36] The electronic spectra of TCNQ and DMTCNQ complexes with the new donors and of TTF–TCNQ are shown in Figure 6. Thus, the highly conducting salts **1a**–TCNQ, **1c**–TCNQ, $(\mathbf{3a})_2$–$(\mathrm{TCNQ})_3$, $(\mathbf{4a})_2$–$(\mathrm{TCNQ})_3$, **1a**–DMTCNQ, and TTF–TCNQ, revealed a broad and intense absorption at the wavenumber ($\tilde{\nu}$) of 3–4 kcm^{-1}, which can be assigned as a mixed-valence transition characteristic of the segregated stacking structure of donor and acceptor components. On the other hand, for the poorly conducting DMTCNQ salts of **1c**, **3a**, and **4a** the absorptions appear at higher energy (ca. 6 kcm^{-1}). These absorptions are typical of a charge-transfer transition in an alternating donor–acceptor stacking arrangement.

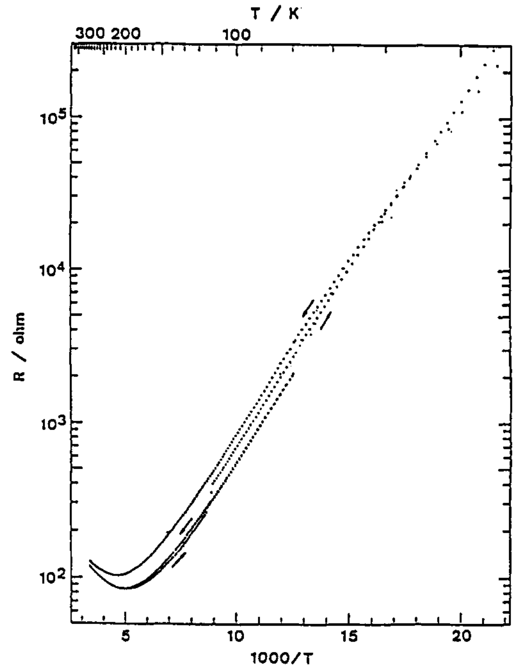

Figure 7. Plots of resistance (R, Ω) with respect to $1000/T$ (K^{-1}) in **1a**-TCNQ single crystals.

Single Crystals of 1a–TCNQ. The single crystals of **1a**–TCNQ complex were prepared by using a diffusion technique in a quartz vessel equipped with three chambers, each of which was filled with anisole. The largest single crystals were $3 \times 0.05 \times 0.05$ mm^3. X-ray crystallographic analysis of these crystals was unsuccessful. The electric resistance of the crystals was measured by a four-probe method in the temperature range 300–48 K (Figure 7). The electric conductivity at 300 K was 16 S/cm, and the value gradually increased as the temperature decreased from 300 to ca. 200 K, thus reaching a maximum of 23 S/cm. This change of electric conductivity with temperature implies that the crystals are metallic in this temperature range. However, near 200 K, a metal-to-insulator phase transition occurred, and below this temperature, semiconductive behavior was observed. It is not yet clear whether the phase transition is a "Peierls transition" or not.[37]

Acknowledgment. We thank Professor H. Inokuchi, Dr. T. Enoki, and Dr. K. Imaeda (Institute of Molecular Science) and Professor I. Tsujikawa and Dr. H. Kobayashi (Kyoto University) for their kind help with the electric conductivity measurements. This work was partially supported by a Grand-In-Aid for the Special Project Research on the Properties of Molecular Assemblies (No. 58118002) and Grand-In-Aid for the Developmental Scientific Research (No. 59850140) from the Ministry of Education, Science and Culture.

---

(36) Torrance, J. B.; Scott, B. A.; Kaufman, F. B. *Solid State Commun.* **1975**, *17*, 1369.

(37) Peierls, R. E. *Quantum Theory of Solids* 1955, Clarendon Press, Oxford.